

Functional delta residuals and applications to simultaneous confidence bands of moment based statistics

Fabian J.E. Telschow^{1,*}, Samuel Davenport² and Armin Schwartzman^{2,3}

¹Institute of Mathematics, Humboldt Universität zu Berlin

²Division of Biostatistics, University of California, San Diego

³Halicioğlu Data Science Institute, University of California, San Diego

February 24, 2022

Abstract

Given a functional central limit (fCLT) for an estimator and a parameter transformation, we construct random processes, called functional delta residuals, which asymptotically have the same covariance structure as the limit process of the functional delta method. An explicit construction of these residuals for transformations of moment-based estimators and a multiplier bootstrap fCLT for the resulting functional delta residuals are proven. The latter is used to consistently estimate the quantiles of the maximum of the limit process of the functional delta method in order to construct asymptotically valid simultaneous confidence bands for the transformed functional parameters. Performance of the coverage rate of the developed construction, applied to functional versions of Cohen's d, skewness and kurtosis, is illustrated in simulations and their application to test Gaussianity is discussed.

1 Introduction

Recently there has been an increased interest in modeling functional data in the Banach space $C(S)$ of continuous functions endowed with the supremum norm, as, unlike Hilbert space methods based on integral norms such as the L^2 -norm, it allows for relevant differences to be localized and tested. This approach was pioneered in Dette et al. [2020], Dette and Kokot [2020] for functional time series data. Results regarding functional data in the subspace of C^3 -processes of the Banach space $C(S)$ have notably been applied, primarily via the framework of random field theory, in order to control the familywise error rate for smooth test statistics over continuous compact domains (see e.g., Adler [1981], Worsley et al. [2004], Taylor and Worsley [2007]). Furthermore, analysis of functional data in the context of $C(S)$ is key in the construction of simultaneous confidence bands for the mean function or its derivatives [Degras, 2011, Cao et al., 2012, Cao, 2014, Chang et al., 2017, Wang et al., 2019, Telschow and Schwartzman, 2022, Liebl and Reimherr, 2019]. Other emerging applications include simultaneous confidence bands for covariance functions [Cao et al., 2016, Wang et al., 2020], testing for equality of covariance functions using the supremum norm Guo et al. [2018], Confidence Probability Excursion (CoPE) sets [Sommerfeld et al., 2018] and techniques to detect relevant differences in the mean and covariance functions of two samples Dette and Kokot [2020, 2021].

*Corresponding author: fabian.telschow@hu-berlin.de, Rudower Chaussee 25, 12489 Berlin, Germany

Non-linear functional parameters, with the notable exception of the covariance function, have not yet received much attention in the context of $C(S)$ random variables. This article will provide insight into this topic by introducing a construction of residuals – called functional delta residuals – which can be used to simulate from the limiting Gaussian field of a non-linear statistic over an arbitrary compact domain. We will use this to construct asymptotic simultaneous confidence bands for moment-based statistics, such as Cohen’s d , skewness and kurtosis, which are differentiable functions of pointwise moments of the data.

The motivation for our work comes from the following problem in spatial functional data analysis. Sommerfeld et al. [2018], in the context of climate data, and Bowring et al. [2019], in the context of functional magnetic resonance imaging, study confidence statements about excursion sets of the mean function $\mu(s)$ from a sample $Y_1(s), \dots, Y_N(s)$ observed from a signal plus noise model $Y(s) = \mu(s) + \varepsilon(s)$. Here $\varepsilon(s)$ is a stochastic error process with variance function $\sigma^2(s)$ and s is a spatial index in a compact set $S \subset \mathbb{R}^D$. Their method requires estimation of the quantiles of the maximum of a limiting Gaussian process. These quantiles are estimated from the residuals $Y_n - \bar{Y}$ through a multiplier bootstrap [Chang and Ogden, 2009, Chang et al., 2017] or the Gaussian kinematic formula [Worsley et al., 2004, Adler and Taylor, 2009]. These methods successfully approximate the quantiles since the empirical covariance structure estimated from these residuals, asymptotically, has the same covariance structure as the limiting Gaussian process of $\sqrt{N}(\bar{Y} - \mu)$. Unsurprisingly, this approach no longer works if the object of interest is a non-linear transformation H of the parameters, since the limiting Gaussian process of $\sqrt{N}(H(\bar{Y}) - H(\mu))$ in general has a different covariance structure than the residuals $Y_n - \bar{Y}$, compare Figure 1 and 2. However, it is not immediately clear how to obtain residuals with the correct correlation structure, because applying the non-linear transformation to the residuals directly does not provide the correct correlation structure. In order to solve this problem we introduce the concept of functional delta residuals.

Our main result, Theorem 1, shows that functional delta residuals have the same asymptotic covariance structure as the limiting process from the fCLT for the transformed estimator. As an application, we derive the functional delta residuals for moment-based statistics such as the functional Cohen’s d , skewness and kurtosis. Therefore we need to show that fCLTs in the Banach space of continuous functions hold for vectors of sample moments (Theorem 2) which in particular implies that they hold for moment-based statistics Corollary 1(a). The resulting functional delta residuals for moment-based statistics will be derived in Section 3.2. In Theorem 3 we provide a conditional multiplier functional limit theorem using these residuals, which we prove using similar arguments to those used in Kosorok [2003] and Chang and Ogden [2009]. In Theorem 4 we show that combining the previous results it is possible to construct asymptotic simultaneous confidence bands for moment-based statistics. In particular the theory developed in our article provides a rigorous justification for the methods that we developed in Bowring et al. [2021]. In that paper we extended our previous work on CoPE sets of signals in fMRI experiments to spatial inference using CoPE sets for Cohen’s d , a statistic which important for measuring the power of a test, see Davenport and Nichols [2020]. Moreover, we demonstrate how a transformation of pointwise skewness and kurtosis can be used to test Gaussianity of $C(S)$ -valued samples. This uses transformations which transform the skewness and kurtosis estimators to have approximately standard normal distributions D’agostino et al. [1990]. In order to incorporate these results it is necessary to extend the theory to work also for transformations depending on H_N . This mainly requires an extension of the Delta method to transformations depending on N which is proven in 6.

The paper is organized as follows: Section 2 introduces the general concept of functional delta residuals. Section 3 shows how to apply the general concept to moment-based statistics

and includes the statements and proofs of our main results. Section 4 studies the performance of simultaneous confidence bands for Cohen’s d , skewness, kurtosis and certain transformations of skewness and kurtosis.

The proposed methods for simultaneous confidence bands are implemented in the R-package SIRF (Spatial Inference for Random Fields) available at <https://github.com/ftelschow/SIRF>. Code reproducing the simulations is available at <https://github.com/ftelschow/SIRF/DeltaResiduals>.

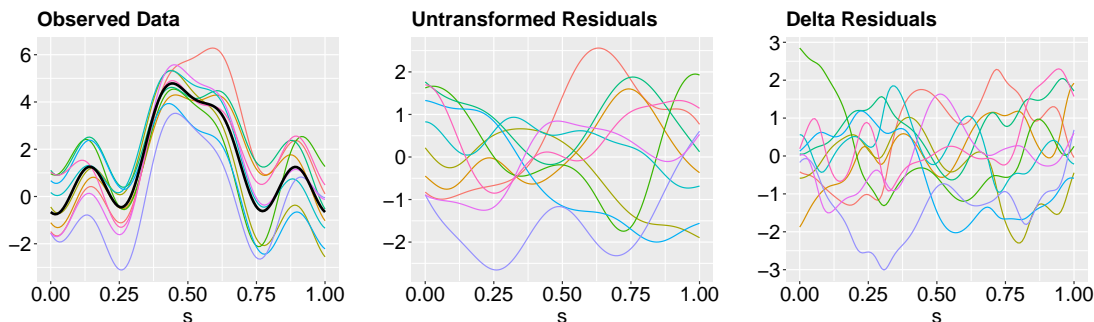


Figure 1: **Left:** samples of a Gaussian process with square exponential covariance function with a linear combination of Gaussian densities as mean (bold black line). **Middle:** the untransformed residuals of this process. **Right:** the functional delta residuals of Cohen’s d of this process.

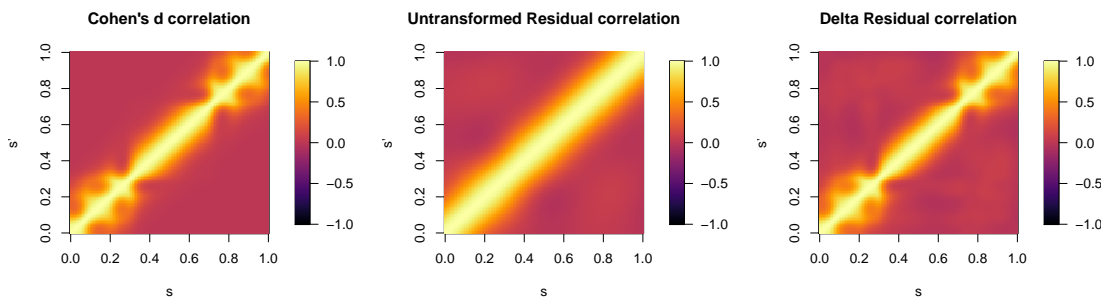


Figure 2: **Left:** the true asymptotic correlation function of Cohen’s d as given in Corollary 2 of the same process. **Middle:** correlation structure estimated from the sample correlation of a sample of untransformed residuals of size 100. **Right:** correlation structure of Cohen’s d estimated from the sample correlation of a sample of delta residuals of size 100.

2 Functional Delta Residuals

In this section we introduce the construction of functional delta residuals. Throughout the article $C^k(S, \mathbb{R}^P)$, $k, P \in \mathbb{N}$, denotes the space of k -times continuously differentiable functions with values in \mathbb{R}^P and domain S . For ease of readability $C^k(S, \mathbb{R})$ will be denoted by $C^k(S)$. We develop delta residuals in the framework of the Banach space $C(S, \mathbb{R}^P)$ of continuous functions with values in \mathbb{R}^P over a compact domain $S \subseteq \mathbb{R}^D$, $D \in \mathbb{N}$. However the concept can be extended to other Banach spaces of functions and more general domains. The norm on $C(S, \mathbb{R}^P)$ is the maximum norm $\|f\|_\infty = \max_{s \in S} |f(s)|$, where $|\cdot|$ denotes the standard

norm on \mathbb{R}^P . The notation " \rightsquigarrow " will denote weak convergence in $C(S, \mathbb{R}^P)$, while a bold symbol denotes a vector. Moreover, $\mathbf{v}^T \in \mathbb{R}^{1 \times P}$ denotes the transpose of a column vector $\mathbf{v} \in \mathbb{R}^P$. Given a function f from $S \times S$ to \mathbb{R} we will write $f(s, s')$ to refer to f evaluated at $s, s' \in S$ without explicitly defining s, s' . Under this more general setup since a purely formal treatment hides the basic idea behind delta residuals, we motivate them with a special case. Let $\{X_n\}_{n \in \mathbb{N}}$ be a sequence of random processes in $C(S)$ such that all elements are independent and identically distributed as X with $\mathbf{c}(s, s') = \text{Cov}[X(s), X(s')] < \infty$ for all $s, s' \in S$ and $\mu = \mathbb{E}[X]$. Assume that this array satisfies a functional CLT, i.e.,

$$\sqrt{N}(\bar{X}_N - \mu) = \frac{1}{\sqrt{N}} \left(\sum_{n=1}^N X_n - \mu \right) \rightsquigarrow G, \quad (1)$$

where $\bar{X}_N = N^{-1} \sum_{n=1}^N X_n$ is the sample mean and G is a tight zero-mean Gaussian process in $C(S)$ with covariance function \mathbf{c} . Assume further that the residuals $R_{N,n} = X_n - \bar{X}_N$ satisfy

$$\lim_{N \rightarrow \infty} \frac{1}{N} \sum_{n=1}^N R_{N,n}(s) R_{N,n}(s') = \mathbf{c}(s, s'). \quad (2)$$

almost surely for all $s, s' \in S$. For reasons which become clear in the next step we call the residuals $R_{N,1}, \dots, R_{N,N}$ the untransformed residuals.

Let $H \in C^1(\mathbb{R})$ and denote with dH_x the derivative of H at $x \in \mathbb{R}$. Suppose we are interested in inferring on the function $s \mapsto H(\mu(s))$. Then Equations (1) and (2) imply that the transformed processes $\tilde{R}_{N,n}(s) = dH_{\bar{X}_N(s)} R_{N,n}(s)$, which we call functional delta residuals (delta residuals for short), satisfy

$$\begin{aligned} \lim_{N \rightarrow \infty} \frac{1}{N} \sum_{n=1}^N \tilde{R}_{N,n}(s) \tilde{R}_{N,n}(s') &= \lim_{N \rightarrow \infty} dH_{\bar{X}_N(s)} dH_{\bar{X}_N(s')} \frac{1}{N} \sum_{n=1}^N R_{N,n}(s) R_{N,n}(s') \\ &= dH_{\mu(s)} \mathbf{c}(s, s') dH_{\mu(s')} \end{aligned}$$

almost surely for all $s, s' \in S$. They can thus be used to approximate the covariance structure of \tilde{G} , which is the Gaussian limiting process appearing in the fCLT obtained from the delta residuals method, since

$$\sqrt{N} \left(H(\bar{X}_N) - H(\mu) \right) \rightsquigarrow \tilde{G} = dH_{\mu} G.$$

The next result generalizes the outlined concept of functional delta residuals to arbitrary functional estimators $\hat{\theta}_N$ and clarifies some of the underlying necessary conditions.

Theorem 1. *Let $N \in \mathbb{N}$ and $\hat{\theta}_N \in C(S, \mathbb{R}^P)$ be an estimator of a parameter $\theta \in C(S, \mathbb{R}^P)$ such that as $N \rightarrow \infty$*

$$\sqrt{N} \left(\hat{\theta}_N - \theta \right) \rightsquigarrow \mathbf{G}, \quad (3)$$

weakly in $C(S, \mathbb{R}^P)$, where \mathbf{G} denotes a zero-mean Gaussian process on $C(S, \mathbb{R}^P)$ with covariance function \mathbf{c} . Let $H \in C^1(\mathbb{R}^P, \mathbb{R}^{P'})$ then

(a) *the functional delta method implies that*

$$\sqrt{N} \left(H(\hat{\theta}_N) - H(\theta) \right) \rightsquigarrow dH_{\theta} \mathbf{G} = \tilde{\mathbf{G}}, \quad N \rightarrow \infty$$

where dH_x is the derivative of H at $x \in \mathbb{R}^P$ and $\tilde{\mathbf{G}}$ is a zero-mean Gaussian process with covariance $\tilde{\mathbf{c}}(s, s') = dH_{\theta(s)} \mathbf{c}(s, s') dH_{\theta(s')}^T$,

(b) if $\{\mathbf{R}_{N,n} : N \in \mathbb{N}, 1 \leq n \leq N\}$ is a triangular array of random processes in $C(S, \mathbb{R}^P)$ such that $\sum_{n=1}^N \mathbf{R}_{N,n} = 0$ and

$$\lim_{N \rightarrow \infty} N^{-1} \sum_{n=1}^N \mathbf{R}_{N,n}(s) \mathbf{R}_{N,n}^T(s') = \mathbf{c}(s, s') \in \mathbb{R}^{P \times P}. \quad (4)$$

uniformly in probability, then the functional delta residuals $\tilde{\mathbf{R}}_{N,n}(s) = dH_{\hat{\boldsymbol{\theta}}_N(s)} \mathbf{R}_{N,n}(s)$, $n = 1, \dots, N$, satisfy

$$\lim_{N \rightarrow \infty} N^{-1} \sum_{n=1}^N \tilde{\mathbf{R}}_{N,n}(s) \tilde{\mathbf{R}}_{N,n}^T(s') = \tilde{\mathbf{c}}(s, s')$$

uniformly in probability and $\sum_{n=1}^N \tilde{\mathbf{R}}_{N,n} = 0$.

Proof. Part (a) is a simple Taylor expansion argument showing that H , considered as a function of $C(S, \mathbb{R}^P) \rightarrow C(S, \mathbb{R}^{P'})$, is Hadamard differentiable tangential to $C(S, \mathbb{R}^P)$. Thus [Kosorok, 2008, Theorem 2.8] implies that the delta method is applicable, which proves (a).

To prove (b) note that, by linearity of the differential,

$$N^{-1} \sum_{k=1}^N \tilde{\mathbf{R}}_{N,n}(s) \tilde{\mathbf{R}}_{N,n}^T(s') = dH_{\hat{\boldsymbol{\theta}}_N(s)} \left(N^{-1} \sum_{k=1}^N \mathbf{R}_{N,n}(s) \mathbf{R}_{N,n}^T(s') \right) dH_{\hat{\boldsymbol{\theta}}_N(s')}^T. \quad (5)$$

The fCLT (3) implies that $\hat{\boldsymbol{\theta}}_N \rightarrow \boldsymbol{\theta}$ uniformly in probability. Additionally, $dH_{\hat{\boldsymbol{\theta}}_N(s)} \rightarrow dH_{\boldsymbol{\theta}(s)}$ uniformly in probability as $N \rightarrow \infty$, by the continuous mapping theorem, and so the claim follows from (5). \square

Remark 1. Two observations are noteworthy. Firstly, the factors \sqrt{N} in equation (3) and N^{-1} in equation (4) can be replaced by general factors tending to infinity and zero respectively provided they are also changed in the subsequent equations (we stick to these factors here in order to keep the notation simple). Secondly, if $dH_{\boldsymbol{\theta}(s)} = 0$ for all $s \in S$, then the delta residuals can be identically equal to zero. In that case an assumption of higher differentiability of H can be used to establish a similar result using a second-order delta method.

3 Delta Residuals for Moment-based Statistics

In this section we illustrate how Theorem 1 can be applied to statistics based on differentiable functions of pointwise sample moments which we call moment-based statistics. Hereafter, unless otherwise stated, we assume that $\{X_n\}_{n \in \mathbb{N}}$ is a sequence of random processes in $C(S)$ such that all elements are independent and identically distributed as X . For $r \in \mathbb{N}$, the r -th pointwise population moment of X is defined by $\mu^{(r)}(s) = \mathbb{E}[X^r(s)]$ and the (non-centered) sample moment as

$$\hat{\mu}_N^{(r)}(s) = \frac{1}{N} \sum_{n=1}^N X_n^r(s).$$

Statistics such as Cohen's d , skewness or kurtosis can be expressed as continuously differentiable functions of the sample moments and therefore functional delta residuals for these statistics can be constructed from the general framework described below. Specific examples will be discussed in Section 3.3.

3.1 A Functional Central Limit Theorem for Moments

In order to apply Theorem 1 we need to establish a fCLT for vectors of different sample moments $\hat{\mu}_N^{(r)}$. We base the proof of our fCLT on the following sample path property for the process X . However, other properties allowing for fCLTs could be used.

Definition 1. Let Y be a process in $C(S)$. Given $p \in \mathbb{N}$, we say that Y has \mathcal{L}^p -Hölder continuous paths of order $\alpha \in (0, 1]$, if

$$|Y(s) - Y(s')| \leq L |s - s'|^\alpha \quad (6)$$

almost surely for all $s, s' \in S$ with L a positive random variable satisfying $\mathbb{E}[L^p] < \infty$.

Remark 2. \mathcal{L}^2 -Hölder continuous paths ensure that Y satisfies a fCLT, i.e., for $Y, Y_1, \dots, Y_N, \dots$ an i.i.d. sequence in $C(S)$, the sum $N^{-1/2} \sum Y_n$ converges weakly to a tight zero-mean Gaussian process which has the same covariance structure as Y , see [Jain and Marcus \[1975, Theorem 1\]](#). Similar fCLTs for dependent functional arrays requiring a mixing condition have been recently shown in [Dette et al. \[2020, Theorem 2.1\]](#).

Remark 3. It is obvious that Y satisfies a fCLT, eq. (1), if Y is a Gaussian process. However, it is still interesting to note that if Y has almost surely C^1 -sample paths, then applying [[Landau and Shepp, 1970, Theorem 4](#)] to the components of the gradient process implies that Y has \mathcal{L}^p -Hölder continuous paths for any $p \in \mathbb{N}$.

The following Lemma states useful properties of processes with \mathcal{L}^p -Hölder continuous paths and is an adaptation Lemma 5 of [Telschow and Schwartzman \[2022\]](#).

Lemma 1. *Let $\{Y_n\}_{n \in \mathbb{N}} \sim Y$ be i.i.d. processes in $C(S)$ and $\{Z_n\}_{n \in \mathbb{N}} \sim Z$ be i.i.d. processes in $C(S)$ such that Z and Y both have \mathcal{L}^p -Hölder continuous paths with $p \geq 1$ and the domain S is compact. Assume that there exist $s', s'' \in S$ such that $\mathbb{E}[|Y(s')|^p]$ and $\mathbb{E}[|Z(s'')|^p]$ are finite. Then*

- (a) $\mathbb{E}[\|Y\|_\infty^q] < \infty$ for all $q \leq p$.
- (b) $\|\bar{Y}_N - \mathbb{E}[Y]\|_\infty \rightarrow 0$ almost surely as N tends to infinity.
- (c) If $p \geq 2$, then $\|N^{-1} \sum_{n=1}^N (Y_n - \bar{Y}_N)(Z_n - \bar{Z}_N) - \text{Cov}[Y, Z]\|_\infty \rightarrow 0$ almost surely as N tends to infinity. Here $\|\cdot\|_\infty$ denotes the maximum norm on $C(S \times S)$.

Proof. Proof of (a): Using the convexity of $|\cdot|^p$, $\mathbb{E}[|Y(s')|^p] < \infty$ and $\delta(s, s') = |s - s'|^\alpha$ we have

$$\begin{aligned} \mathbb{E}[\|Y\|_\infty^p] &\leq 2^{p-1} \left(\mathbb{E}[\|Y - Y(s')\|_\infty^p] + \mathbb{E}[|Y(s')|^p] \right) \\ &\leq 2^{p-1} \left(\mathbb{E}[L^p] \max_{s \in S} \delta(s, s') + \mathbb{E}[|Y(s')|^p] \right), \end{aligned}$$

where L is the random variable from the \mathcal{L}^p -Hölder property. This yields $\mathbb{E}[\|Y\|_\infty^q] < \infty$ for all $q \leq p$.

Proof of (b): We apply the generic uniform convergence result in [Davidson \[1994, Theorem 21.8\]](#). Since pointwise convergence holds by the strong law of large numbers, it is sufficient to

establish strong stochastic equicontinuity of the random function $\bar{Y}_N - \mathbb{E}[Y]$. This is established using [Davidson \[1994, Theorem 21.10 \(ii\)\]](#), since

$$|\bar{Y}_N(s) - \bar{Y}_N(s') - \mathbb{E}[Y(s) - Y(s')]| \leq \left(\sum_{n=1}^N \frac{L_n}{N} + \mathbb{E}[L] \right) \delta(s, s') = C_N \delta(s, s')$$

for all $s, s' \in S$. Here $L_1, \dots, L_N \sim L$ i.i.d. denote the random variables from the \mathcal{L}^p -Hölder paths of the Y_n 's and Y . Hence the random variable C_N converges almost surely to the constant $2\mathbb{E}[L]$ by the strong law of large numbers.

Proof of (c): First we have that, for all $s, s' \in S$,

$$\begin{aligned} |Y_n(s) - \bar{Y}_N(s) - Y_n(s') + \bar{Y}_N(s')| &\leq |Y_n(s) - Y_n(s')| + |\bar{Y}_N(s') - \bar{Y}_N(s)| \\ &\leq \left(L_n + \frac{1}{N} \sum_{n=1}^N L_n \right) \delta(s, s') \\ &\leq K_n \delta(s, s'), \end{aligned}$$

where $L_n, n \in \{1, \dots, N\}$, is the random \mathcal{L}^p -Hölder constant of Y_n . Therefore $A_n = Y_n - \bar{Y}_N$ has \mathcal{L}^2 -Hölder paths since $p \geq 2$. The same holds for $B_n = Z_n - \bar{Z}_N$. Hence we compute

$$\begin{aligned} &\left| \frac{1}{N} \sum_{n=1}^N A_n(s) B_n(t) - A_n(s') B_n(t') \right| \\ &\leq \frac{1}{N} \sum_{n=1}^N \|A_n\|_\infty \tilde{K}_n \delta(t, t') + \|B_n\|_\infty K_n \delta(s, s') \\ &\leq \sqrt{\sum_{n=1}^N \frac{\|A_n\|_\infty^2}{N} \sum_{n=1}^N \frac{\tilde{K}_n^2}{N} \delta(t, t')} + \sqrt{\sum_{n=1}^N \frac{\|B_n\|_\infty^2}{N} \sum_{n=1}^N \frac{K_n^2}{N} \delta(s, s')}, \end{aligned}$$

for each $s, s', t, t' \in S$ and $\tilde{K}_1, \dots, \tilde{K}_N$ i.i.d. denote the random variables from the \mathcal{L}^2 -Hölder property of the B_n 's. By the strong law of large numbers the random Hölder constant converges almost surely and is finite. Thus, again the generic uniform convergence result in [Davidson \[1994, Theorem 21.8\]](#) together with [Davidson \[1994, Theorem 21.10\]](#) yield the claim. \square

To handle vector-valued random processes, we require the following Lemma in order to prove [Theorem 2](#). This states simple conditions for obtaining weak convergence of a vector-valued process from its components. Its generalization to arbitrary dimensional vector-valued processes is immediate.

Lemma 2. *Let $X_1, X_2, \dots, X, Y_1, Y_2, \dots, Y$ be $C(S)$ -valued random variables on the probability space $(\Omega, \mathcal{F}, \mathbb{P})$ such that $X_N \rightsquigarrow X$ and $Y_N \rightsquigarrow Y$. If the finite dimensional distributions of (X_N, Y_N) converge to those of (X, Y) , we have $(X_N, Y_N) \rightsquigarrow (X, Y)$ in $C(S) \times C(S)$.*

Proof. Tightness of the pair (X_N, Y_N) is implied by [Lemma 1.4.3](#) and [Problem 9](#) in [Section 1.3](#) from [Van Der Vaart and Wellner \[1996\]](#) (hereafter VW).

Moreover, the finite dimensional distributions converge and form a separating class in $C(S) \times C(S)$ (the proof is along the lines of [Example 1.3](#) in [\[Billingsley, 1999, p. 12\]](#)) so in particular the joint distribution converges (arguing as in [Example 5.1](#) in [\[Billingsley, 1999, p. 57\]](#)). \square

With these preparatory results we can now prove the main theorem of this section.

Theorem 2. *Let S be a compact space and $\{X_n\}_{n \in \mathbb{N}}$ be i.i.d. processes in $C(S)$ distributed as X . Let $r_1, \dots, r_K \in \mathbb{N}$ such that $1 < r_1 < \dots < r_K$, for some $K \in \mathbb{N}$. Denote the corresponding vector as $\mathbf{r} = (r_1, \dots, r_K)$. Assume that X has \mathcal{L}^{2r_K} -Hölder continuous paths with L the random Hölder bound and there exists an $s \in S$ such that $\mathbb{E}[X^{2r_K}(s)] < \infty$. Then*

$$\sqrt{N} \left(\hat{\boldsymbol{\mu}}_N^{(\mathbf{r})} - \boldsymbol{\mu}^{(\mathbf{r})} \right) \rightsquigarrow \mathbf{G}. \quad (7)$$

Here $\hat{\boldsymbol{\mu}}_N^{(\mathbf{r})} = \left(\hat{\mu}_N^{(r_1)}, \dots, \hat{\mu}_N^{(r_K)} \right)$ and $\boldsymbol{\mu}^{(\mathbf{r})} = \left(\mu^{(r_1)}, \dots, \mu^{(r_K)} \right)$. Moreover, \mathbf{G} is a zero-mean Gaussian process with paths in $C(S, \mathbb{R}^K)$ and covariance matrix function \mathbf{c} having entries

$$\mathbf{c}_{kl}(s, s') = \mathbb{E}[X^{r_k}(s) X^{r_l}(s')] - \mu^{(r_k)}(s) \mu^{(r_l)}(s') \quad \text{for } k, l = 1, \dots, K, \text{ and } s, s' \in S.$$

Proof. First we need to establish that for all $k = 1, \dots, K$ the sequence $\{X_n^{r_k}\}_{n \in \mathbb{N}}$ satisfy the CLT in $C(S)$. To do so observe that for all x, y we have that $|x^{r_k} - y^{r_k}| \leq (r_k - 1) \max_{\xi \in \{x, y\}} \xi^{r_k-1} |x - y|$, since we can factor as

$$\begin{aligned} x^{r_k} - y^{r_k} &= (x - y) \sum_{l=0}^{r_k-1} x^{r_k-1-l} y^l \leq (x - y) (r_k - 1) x^{r_k-1}, \quad \text{for } x \geq y \\ y^{r_k} - x^{r_k} &= (y - x) \sum_{l=0}^{r_k-1} y^{r_k-1-l} x^l \leq (y - x) (r_k - 1) y^{r_k-1}, \quad \text{for } y \geq x. \end{aligned}$$

Hence

$$\begin{aligned} |X^{r_k}(s) - X^{r_k}(s')| &\leq (r_k - 1) \max_{s \in S} |X(s)|^{r_k-1} |X(s) - X(s')| \\ &\leq (r_k - 1) L \|X\|_{\infty}^{r_k-1} |s - s'|^\alpha. \end{aligned} \quad (8)$$

Using Hölder's inequality for $p = r_k$ and $q = r_k / (r_k - 1)$ we obtain for all $k = 1, \dots, K$ that

$$\mathbb{E} \left[L^2 \|X\|_{\infty}^{2(r_k-1)} \right] \leq \mathbb{E} \left[L^{2r_k} \right]^{\frac{1}{r_k}} \mathbb{E} \left[\|X\|_{\infty}^{2r_k} \right]^{\frac{r_k-1}{r_k}} < \infty$$

by Lemma 1(a) applied to X . As such the positive random variable $M = (r_k - 1) L \|X\|_{\infty}^{r_k-1}(s)$ satisfies $\mathbb{E}[M^2] < \infty$ and the fCLT for each $k = 1, \dots, K$ follows from Jain and Marcus [1975, Theorem 1].

In order to apply Lemma 2 it remains to show that the finite dimensional distributions converge to the finite dimensional distributions of \mathbf{G} from the statement of the theorem. To see this, for $s \in S$, define $\mathbf{X}_n^{(\mathbf{r})}(s) = (X_n^{r_1}(s), \dots, X_n^{r_K}(s))$ and $\boldsymbol{\mu}^{(\mathbf{r})}(s) = (\mu^{r_1}(s), \dots, \mu^{r_K}(s))$. For $I \in \mathbb{N}$ and any $s_1, \dots, s_I \in S$, we apply the multivariate CLT to the sequence of random vectors

$$\left(\mathbf{X}_n^{(\mathbf{r})}(s_1) - \boldsymbol{\mu}^{(\mathbf{r})}(s_1), \dots, \mathbf{X}_n^{(\mathbf{r})}(s_I) - \boldsymbol{\mu}^{(\mathbf{r})}(s_I) \right),$$

which yields convergence to the finite dimensional distributions of a Gaussian random vector with covariance matrix $\Sigma \in \mathbb{R}^{KI \times KI}$ given by

$$\begin{aligned} \Sigma_{i \cdot K+k, j \cdot K+l} &= \text{Cov} \left[X^{r_k}(s_i) - \mu^{(r_k)}(s_i), X^{r_l}(s_j) - \mu^{(r_l)}(s_j) \right] \\ &= \mathbb{E} \left[X^{r_k}(s_i) X^{r_l}(s_j) \right] - \mu^{(r_k)}(s_i) \mu^{(r_l)}(s_j), \end{aligned}$$

for $i, j = 1, \dots, I - 1$ and $k, l = 1, \dots, I$. Hence these finite dimensional distributions converge to those of \mathbf{G} , which finishes the proof. \square

Remark 4. During the proof of the previous theorem we showed in eq. (8) that if X has \mathcal{L}^{2r} -Hölder continuous paths and there exist an $s \in S$ such that $\mathbb{E}[X^{2r}(s)] < \infty$ then X^r has \mathcal{L}^2 -Hölder continuous paths.

3.2 Delta Residuals

In the previous section we established a multivariate functional CLT for sample moments. In order to apply Theorem 1 we must construct untransformed residuals having the covariance structure given in Theorem 2.

Proposition 1 (Moment Residuals). *We call the processes $R_{N,n}^{(r)} = X_n^r - \hat{\mu}_N^{(r)}$ the r -th moment residuals, which satisfy $\sum_{n=1}^N R_{N,n}^{(r)} = 0$. Let $r_1, r_2 \in \mathbb{N}$ and assume that X has $\mathcal{L}^{2\max(r_1, r_2)}$ -Hölder continuous paths, then*

$$\lim_{N \rightarrow \infty} N^{-1} \sum_{n=1}^N R_{N,n}^{(r_1)}(s) R_{N,n}^{(r_2)}(s') = \mathbb{E} [X^{r_1}(s) X^{r_2}(s')] - \mu^{(r_1)}(s) \mu^{(r_2)}(s'), \quad s, s' \in S \quad (9)$$

almost surely uniformly in $C(S \times S)$.

Proof. The r -th moment residuals sum to zero by construction. By Lemma 1(c) and Remark 4 it follows that, if $s, s' \in S$,

$$\begin{aligned} N^{-1} \sum_{n=1}^N R_{N,n}^{(r_1)}(s) R_{N,n}^{(r_2)}(s') &= N^{-1} \sum_{n=1}^N (X_n^{r_1}(s) - \hat{\mu}_N^{(r_1)}(s)) (X_n^{r_2}(s') - \hat{\mu}_N^{(r_2)}(s')) \\ &\xrightarrow{N \rightarrow \infty} \text{Cov}[X^{r_1}(s), X^{r_2}(s')] \\ &= \mathbb{E} [X^{r_1}(s) X^{r_2}(s')] - \mu^{(r_1)}(s) \mu^{(r_2)}(s') \end{aligned}$$

uniformly almost surely in $C(S \times S)$. \square

Combining the fCLT for vectors of moments, Theorem 2, and the above Proposition 1, which shows that moment residuals can play the role of the untransformed residuals in Theorem 1, we obtain the following corollary.

Corollary 1. *Assume the assumptions of Theorem 2 and assume that $H \in C^1(\mathbb{R}^K)$. Then*

(a) *Let \tilde{G} be a zero-mean Gaussian process with covariance*

$$\tilde{\mathbf{c}}(s, s') = dH_{\boldsymbol{\mu}^{(r)}(s)} \mathbf{c}(s, s') dH_{\boldsymbol{\mu}^{(r)}(s')}^T,$$

where $\mathbf{c}(s, s')$ is given in Theorem 2. Then

$$\sqrt{N} \left(H(\hat{\boldsymbol{\mu}}_N^{(r)}) - H(\boldsymbol{\mu}^{(r)}) \right) \rightsquigarrow \tilde{G}, \quad N \rightarrow \infty. \quad (10)$$

(b) *The delta residuals*

$$\tilde{R}_{N,n}^{(r)} = dH_{\hat{\boldsymbol{\mu}}_N^{(r)}} \mathbf{R}_{N,n}^{(r)}, \quad n = 1, \dots, N, \quad (11)$$

where $\mathbf{R}_{N,n}^{(r)} = \left(R_{N,n}^{(r_1)}, \dots, R_{N,n}^{(r_K)} \right)^T$, satisfy

$$\lim_{N \rightarrow \infty} N^{-1} \sum_{n=1}^N \tilde{R}_{N,n}(s) \tilde{R}_{N,n}^T(s') = \tilde{\mathbf{c}}(s, s') \quad (12)$$

uniformly almost surely in $C(S \times S)$.

3.3 Examples of Delta Residuals Based on Moments

We will now discuss a series of examples in which our results can be applied. Throughout this section we will assume that we have a sequence $\{X_n\}_{n \in \mathbb{N}}$ satisfying the assumptions from Theorem 2.

Sample variance. A first simple example of delta residuals can be constructed for the sample variance

$$\hat{\sigma}_N^2(s) = \frac{1}{N} \sum_{n=1}^N \left(X_n(s) - \hat{\mu}_N^{(1)}(s) \right)^2 = \hat{\mu}_N^{(2)}(s) - \left(\hat{\mu}_N^{(1)}(s) \right)^2, \quad (13)$$

which is a uniform almost surely consistent estimator for the pointwise population variance $s \mapsto \text{Var}[X(s)]$. The transformation of $(\mu^{(1)}, \mu^{(2)})$ is given by $H(x, y) = y - x^2$ and the resulting delta residuals are

$$\begin{aligned} R_{N,n}^{\hat{\sigma}_N^2} &= \left(\frac{\partial H}{\partial x} \left(\hat{\mu}_N^{(1)}, \hat{\mu}_N^{(2)} \right), \frac{\partial H}{\partial y} \left(\hat{\mu}_N^{(1)}, \hat{\mu}_N^{(2)} \right) \right) \left(X_n - \hat{\mu}_N^{(1)}, X_n^2 - \hat{\mu}_N^{(2)} \right)^T \\ &= \left(-2\hat{\mu}_N^{(1)}, 1 \right) \left(X_n - \hat{\mu}_N^{(1)}, X_n^2 - \hat{\mu}_N^{(2)} \right)^T \\ &= \left(X_n - \hat{\mu}_N^{(1)} \right)^2 - \hat{\sigma}_N^2. \end{aligned}$$

Cohen's d . Recently, effect size measures gained popularity in the analysis of fMRI data [Bowring et al., 2021, Vandekar and Stephens, 2021]. Bowring et al. [2021] used the pointwise Cohen's d statistic defined by

$$\hat{d}_N(s) = \frac{\hat{\mu}_N^{(1)}(s)}{\sqrt{\hat{\mu}_N^{(2)}(s) - \left(\hat{\mu}_N^{(1)}(s) \right)^2}}, \quad s \in S$$

which is a uniform almost surely consistent estimator for the pointwise population Cohen's d

$$d(s) = \frac{\mu^{(1)}(s)}{\sqrt{\mu^{(2)}(s) - \left(\mu^{(1)}(s) \right)^2}}, \quad s \in S.$$

Note that the denominator will be non-zero, with probability 1 for all $s \in S$, if $N \geq D + 1$ [Adler and Taylor, 2009, Lemma 11.2.10]. The residuals for Cohen's d can be derived from the transformation $H(x, y) = x / \sqrt{y - x^2}$, i.e.,

$$\begin{aligned} R_{N,n}^{\hat{d}_N} &= \left(\frac{\hat{\mu}_N^{(2)}}{\left(\hat{\mu}_N^{(2)} - \left(\hat{\mu}_N^{(1)} \right)^2 \right)^{3/2}}, -\frac{\hat{\mu}_N^{(1)}}{2 \left(\hat{\mu}_N^{(2)} - \left(\hat{\mu}_N^{(1)} \right)^2 \right)^{3/2}} \right) \left(X_n - \hat{\mu}_N^{(1)}, X_n^2 - \hat{\mu}_N^{(2)} \right)^T \\ &= \frac{X_n - \hat{\mu}_N^{(1)}}{\hat{\sigma}_N} - \frac{\hat{d}_N}{2\hat{\sigma}_N^2} \left(\left(X_n - \hat{\mu}_N^{(1)} \right)^2 - \hat{\sigma}_N^2 \right). \end{aligned}$$

Deriving this identity is a little tedious. An elegant shortcut can be taken using the observation that we can treat the residuals $R_n^{\hat{\sigma}_N^2}$ as the untransformed residuals, and use the equivalent

definition for Cohen's d of $\hat{d}_N = \hat{\mu}_N^{(1)} / \sqrt{\hat{\sigma}_N^2}$. Since Theorem 2 together with the delta residuals method applied to the continuously differentiable function $F(x, y) = (x, y - x^2)$ yield a fCLT for the vector valued process $(\hat{\mu}_N^{(1)}, \hat{\sigma}_N^2)$, we can use the transformation $\tilde{H}(x, y) = x / \sqrt{y}$ to obtain

$$\begin{aligned} R_{N,n}^{\hat{d}_N} &= \begin{pmatrix} 1 \\ \hat{\sigma}_N \end{pmatrix}, -\frac{\hat{\mu}_N^{(1)}}{2\hat{\sigma}_N^3} \begin{pmatrix} X_n - \hat{\mu}_N^{(1)}, \left(X_n - \hat{\mu}_N^{(1)} \right)^2 - \hat{\sigma}_N^2 \end{pmatrix}^T \\ &= \frac{X_n - \hat{\mu}_N^{(1)}}{\hat{\sigma}_N} - \frac{\hat{d}_N}{2\hat{\sigma}_N^2} \left(\left(X_n - \hat{\mu}_N^{(1)} \right)^2 - \hat{\sigma}_N^2 \right). \end{aligned}$$

This can also be understood as an application of the chain rule, i.e., $dH_{(x,y)} = d(\tilde{H} \circ F)(x, y) = d\tilde{H}_{F(x,y)} dF_{(x,y)}$. As an illustration of Corollary 1, we derive the asymptotic covariance structure for Cohen's d .

Corollary 2. *Under the assumptions of Theorem 2 we have that $\sqrt{N}(\hat{d}_N(s) - d(s)) \rightsquigarrow \tilde{G}$ with covariance structure $\tilde{\mathbf{c}}$ given by*

$$\tilde{\mathbf{c}}(s, s') = \begin{pmatrix} \sigma(s)^{-1}, -\mu(s)\sigma(s)^{-\frac{3}{2}} \end{pmatrix} \mathbf{c}(s, s') \begin{pmatrix} \sigma(s')^{-1}, -\mu(s')\sigma(s')^{-\frac{3}{2}} \end{pmatrix}^T. \quad (14)$$

Moreover, if X is a Gaussian process, $\tilde{\mathbf{c}}$ simplifies to

$$\tilde{\mathbf{c}}(s, s') = \frac{\mathbf{c}_{11}(s, s')}{\sigma(s)\sigma(s')} + \mathbf{c}_{11}(s, s')^2 \frac{\mu(s)\mu(s')}{2\sigma^3(s)\sigma^3(s')}. \quad (15)$$

Proof. The general form of the covariance structure, i.e., (14), follows by applying Corollary 2. When X is a Gaussian process the asymptotic covariance structure simplifies significantly. To show this, we define $\varepsilon(s) = X(s) - \mu(s)$ and use the fact from the moments of multivariate normal distributions, better known as Isserlis' theorem, cf. Theorem 1 in Vignat [2012],

$$\mathbb{E}[\varepsilon^2(s)\varepsilon^2(s')] = \sigma^2(s)\sigma^2(s') + 2\mathbf{c}_{11}(s, s')^2,$$

for all $s, s' \in S$ to compute

$$\begin{aligned} \mathbf{c}_{22}(s, s') &= \mathbb{E} \left[\left(\varepsilon(s)^2 - \sigma^2(s) \right) \left(\varepsilon(s')^2 - \sigma^2(s') \right) \right] \\ &= \mathbb{E} \left[\varepsilon^2(s)\varepsilon^2(s') \right] - \mathbb{E} \left[\varepsilon^2(s') \right] \sigma(s)^2 - \mathbb{E} \left[\varepsilon^2(s) \right] \sigma^2(s') + \sigma^2(s)\sigma^2(s') \\ &= 2\mathbf{c}_{11}(s, s')^2. \end{aligned}$$

Finally, we note that

$$\mathbf{c}_{12}(s, s') = \mathbb{E} \left[\varepsilon(s) \left(\varepsilon^2(s') - \sigma^2(s') \right) \right] = \mathbb{E} \left[\varepsilon(s)\varepsilon^2(s') \right] = 0 = \mathbf{c}_{21}(s, s'),$$

yielding the simplified version of the limiting covariance structure. \square

Skewness and excess kurtosis. There exist several measures for the skewness and kurtosis of a distribution: a broad overview of these can be found in Joanes and Gill [1998].

Here we will use some of the most standard measures which date back to Fisher [1930]. The skewness estimator is given by

$$g_1^N = \frac{N^{-1} \sum_{n=1}^N \left(X_n - \hat{\mu}_N^{(1)} \right)^3}{\hat{\sigma}_N^3} = \frac{\hat{\mu}_N^{(3)} - 3 \hat{\mu}_N^{(1)} \hat{\mu}_N^{(2)} + 2 \left(\hat{\mu}_N^{(1)} \right)^3}{\left(\hat{\mu}_N^{(2)} - \left(\hat{\mu}_N^{(1)} \right)^2 \right)^{3/2}}. \quad (16)$$

Hence the transformation $H(x, y, z) = (z - 3xy + 2x^3) / (y - x^2)^{3/2}$ together with the first three moment residuals yield functional delta residuals with the correct covariance structure. The sample excess kurtosis can be defined as

$$g_2^N = \frac{N^{-1} \sum_{n=1}^N \left(X_n - \hat{\mu}_N^{(1)} \right)^4}{\hat{\sigma}_N^4} - 3 = \frac{\hat{\mu}_N^{(4)} - 4 \hat{\mu}_N^{(1)} \hat{\mu}_N^{(3)} + \left(\hat{\mu}_N^{(1)} \right)^2 \hat{\mu}_N^{(2)} - 3 \left(\hat{\mu}_N^{(1)} \right)^4}{\left(\hat{\mu}_N^{(2)} - \left(\hat{\mu}_N^{(1)} \right)^2 \right)^2} - 3, \quad (17)$$

which shows that the transformation $H(x, y, z, w) = (w - 4xz + x^2y - 3x^4) / (y - x^2)^2$ together with the first three moment residuals yield functional delta residuals with the correct covariance structure.

3.4 A Multiplier Bootstrap Functional Limit Theorem

We have shown that functional delta residuals can be used to approximate the covariance structure of the limiting process \tilde{G} given in Corollary 1. As such, as we will prove formally in this section, the multiplier bootstrap using the delta residuals can be used to approximate sample path properties of the limiting process. This will, importantly, enable us to estimate the quantiles of the maximum of \tilde{G} . To establish this we prove both weak convergence and the stronger conditional weak convergence VW Chapter 2.6 of the multiplier bootstrap process to \tilde{G} . The main results used in the proof are the Jain-Marcus theorem [Chang and Ogden, 2009, Theorem 1] and Theorem 2 from [Chang and Ogden, 2009].

In the following we assume that $\{g_{N,1}, \dots, g_{N,N} : N \in \mathbb{N}, 1 \leq n \leq N\}$ is a triangular array of i.i.d. random variables defined on the probability space $(\Omega_g, \mathfrak{P}_g, \mathbb{P}_g)$ satisfying $\mathbb{E}[g_{N,1}] = 0$ and $\mathbb{E}[g_{N,1}^2] = 1$. Since the random variables in the sequence $\{X_n\}_{n \in \mathbb{N}}$ are defined on the probability space $(\Omega, \mathfrak{P}, \mathbb{P})$, we define extensions of these random variables to the product space $(\Omega \times \Omega_g, \mathfrak{P} \times \mathfrak{P}_g, \mathbb{P} \otimes \mathbb{P}_g)$ by defining $g_{N,n}(\omega_g, \omega) = g_{N,n}(\omega_g)$ and $X_n(\omega_g, \omega) = X_n(\omega)$ for all $(\omega_g, \omega) \in \Omega \times \Omega_g$.

For $N \geq 1$, the multiplier bootstrap process of the functional delta residuals is defined on the product probability space by

$$\tilde{G}_N^{(g,r)}(\omega_g, \omega) = \frac{1}{\sqrt{N}} \sum_{n=1}^N g_{N,n}(\omega_g) \tilde{R}_{N,n}^{(r)}(\omega), \quad (\omega_g, \omega) \in \Omega \times \Omega_g. \quad (18)$$

The multipliers $g_{N,n}$ and the X_n 's are assumed to be independent on the product space. In particular this means that the $g_{N,n}$ are independent of the functional delta residuals $\tilde{R}_{N,n}^{(r)}$ defined in equation (11). To shorten the notation, given a random variable Y on $(\Omega \times \Omega_g, \mathfrak{P} \times \mathfrak{P}_g, \mathbb{P} \otimes \mathbb{P}_g)$ we define the random variable $Y_\omega = Y(\cdot, \omega)$ on $(\Omega, \mathfrak{P}, \mathbb{P})$ and, in a slight abuse of notation, will also write $X_\omega = X(\omega)$ for a random variable X on $(\Omega, \mathfrak{P}, \mathbb{P})$.

Theorem 3. *Under the assumptions of Theorem 2 the following statements hold*

$$(i) \quad \tilde{G}_N^{(g,r)} \rightsquigarrow \tilde{G} \qquad (ii) \quad \sup_{h \in \mathcal{B}} \left| \mathbb{E}_g \left[h \left(\tilde{G}_N^{(g,r)} \right) \right] - \mathbb{E} \left[h(\tilde{G}) \right] \right| \rightarrow 0.$$

Here convergence in (ii) is in probability with respect to $(\Omega, \mathfrak{F}, \mathbb{P})$, \mathbb{E}_g is the expectation with respect to $(\Omega_g, \mathfrak{F}_g, \mathbb{P}_g)$ and \mathcal{B} is the set of all $h : C(S) \rightarrow \mathbb{R}$ such that $\sup_{f \in C(S)} |h(f)| \leq 1$ and $|h(f) - h(f')| \leq \|f - f'\|_\infty$ for all $s, s' \in S$.

Proof. In order to prove (i) we use the decomposition

$$\begin{aligned} \tilde{G}_N^{(g,r)} &= \frac{1}{\sqrt{N}} \sum_{n=1}^N g_{N,n} dH_{\hat{\mu}_N^{(r)}} \left(\mathbf{X}_n^{(r)} - \hat{\mu}_N^{(r)} \right) \\ &= \mathbf{B}_N \mathbf{X}_N^{(g,r)} + dH_{\mu^{(r)}} \mathbf{X}_N^{(g,r)} + \sqrt{N} \bar{g}_N \mathbf{C}_N, \end{aligned} \tag{19}$$

where $\mathbf{B}_N = dH_{\hat{\mu}_N^{(r)}} - dH_{\mu^{(r)}}$, $\mathbf{X}_N^{(g,r)} = \sum_{n=1}^N \frac{g_{N,n}}{\sqrt{N}} \left(\mathbf{X}_n^{(r)} - \mu^{(r)} \right)$ and $\mathbf{C}_N = dH_{\hat{\mu}_N^{(r)}} \left(\mu^{(r)} - \hat{\mu}_N^{(r)} \right)$.

We first establish that $\mathbf{X}_N^{(g,r)}$ converges weakly to \mathbf{G} from Theorem 2 by using Lemma 2. To do so we demonstrate convergence of the component processes and of the finite dimensional distributions. For weak convergence of the components, it is sufficient to verify conditions (A), (B), (C) and (D) from Chang and Ogden [2009] for the processes $Z_{N,n} = X_n^r / \sqrt{N}$, $r \in \{r_1, \dots, r_K\}$, as the result then follows by applying their Lemma 1 and our Theorem 2. (A) and (C) hold (see the proof of Theorem 2 and the Remark thereafter. For each r , using the convention from Chang and Ogden [2009] that $\{\mathcal{A}\}$ denotes the indicator function of a set \mathcal{A} , we have for every $\eta > 0$ that

$$\sum_{n=1}^N \mathbb{E} \left[\|Z_{N,n}\|_\infty^2 \{ \|Z_{N,n}\|_\infty > \eta \} \right] = \mathbb{E} \left[\|X^r\|_\infty^2 \{ \|X^r\|_\infty > \sqrt{N}\eta \} \right] \xrightarrow{N \rightarrow \infty} 0.$$

This follows by the Dominated Convergence Theorem since by assumption on X we have $\mathbb{E} \left[\|X^r\|_\infty^2 \right] < \infty$ by Lemma 1(a). Thus (B) holds. Condition (D) holds since $\sum_{n=1}^N \mathbb{E} \left[\|Z_{N,n}\|_\infty^2 \right] = \mathbb{E} \left[\|X^r\|_\infty^2 \right] < \infty$. (Note that a square is missing in condition (D) in Chang and Ogden [2009] as can be seen by following the proof of Lemma 1 in Chang and Ogden [2009].) This shows that for each $k \in \{1, \dots, K\}$ the process $N^{-1/2} \sum X_n^{r_k} - \mu^{(r_k)}$ converges weakly in the space $\ell^\infty(S)$ of bounded functions over S to the process given by the k -th component of \mathbf{G} . Since by Theorem 2 the components of \mathbf{G} are $C(S)$ -valued and the sample paths of all $Z_{N,n}$'s are also $C(S)$ -valued, VW's Lemma 1.3.10 establishes weak convergence in $C(S)$ of the component processes. Convergence of the finite dimensional distributions follows directly from the independence of the multipliers and the X_n 's by the multivariate CLT as in Theorem 2. Therefore $\mathbf{X}_N^{(g,r)} \rightsquigarrow \mathbf{G}$ in $C(S, \mathbb{R}^K)$ by Lemma 2. An application of the Continuous Mapping Theorem implies that $dH_{\mu^{(r)}} \mathbf{X}_N^{(g,r)} \rightsquigarrow dH_{\mu^{(r)}} \mathbf{G} = \tilde{G}$. Moreover, \mathbf{B}_N converges uniformly almost surely to zero by Lemma 1 and the Continuous Mapping Theorem. Hence Slutsky's Lemma (VW Example 1.4.7) yields that $\mathbf{B}_N \mathbf{X}_N^{(g,r)}$ converges weakly to zero. The same holds true for $\sqrt{N} \bar{g}_N \mathbf{C}_N$. Combining these observations with the decomposition from eq. (19) it follows that $\tilde{G}_N^{(g,r)} \rightsquigarrow \tilde{G}$ in $C(S)$.

We turn to the proof of (ii). Given $\omega \in \Omega$, consider the decomposition

$$\begin{aligned}
& \sup_{h \in \mathcal{B}} \left| \mathbb{E}_g \left[h \left(\tilde{G}_{N\omega}^{(g,r)} \right) \right] - \mathbb{E} \left[h(\tilde{G}) \right] \right| \\
& \leq \sup_{h \in \mathcal{B}} \left| \mathbb{E}_g \left[h \left(\tilde{G}_{N\omega}^{(g,r)} \right) \right] - \mathbb{E}_g \left[h \left(dH_{\hat{\mu}_{N\omega}^{(r)}} \mathbf{X}_{N\omega}^{(g,r)} \right) \right] \right| \\
& \quad + \sup_{h \in \mathcal{B}} \left| \mathbb{E}_g \left[h \left(dH_{\hat{\mu}_{N\omega}^{(r)}} \mathbf{X}_{N\omega}^{(g,r)} \right) \right] - \mathbb{E} \left[h(\tilde{G}) \right] \right| \\
& \leq \mathbb{E}_g \left[\left\| \tilde{G}_{N\omega}^{(g,r)} - dH_{\hat{\mu}_{N\omega}^{(r)}} \mathbf{X}_{N\omega}^{(g,r)} \right\|_\infty \right] \\
& \quad + \sup_{h \in \mathcal{B}} \left| \mathbb{E}_g \left[h \left(dH_{\hat{\mu}_{N\omega}^{(r)}} \mathbf{X}_{N\omega}^{(g,r)} \right) \right] - \mathbb{E} \left[h(\tilde{G}) \right] \right| \\
& = c \|\mathbf{C}_{N\omega}\|_\infty + \sup_{h \in \mathcal{B}} \left| \mathbb{E}_g \left[h \left(dH_{\hat{\mu}_{N\omega}^{(r)}} \mathbf{X}_{N\omega}^{(g,r)} \right) \right] - \mathbb{E} \left[h(\tilde{G}) \right] \right|
\end{aligned} \tag{20}$$

Here \mathbf{C}_N is defined in the decomposition (19) and $c = \mathbb{E}_g[|\sqrt{N} \bar{g}_N|] < \infty$, which follows from $g_{N,n}$'s being i.i.d. with unit variance. Moreover, since $\|\mathbf{C}_{N\omega}\|_\infty \leq \|dH_{\hat{\mu}_{N\omega}^{(r)}}\|_\infty \|\hat{\mu}_{N\omega}^{(r)} - \mu^{(r)}\|_\infty$ it follows from Lemma 1(b) and the Continuous Mapping Theorem that the first term converges to zero as N tends to infinity for almost all $\omega \in \Omega$.

It remains to show that the second term converges to zero in probability. The proof of the previous part also established that Theorem 2 of Chang and Ogden [2009] is applicable to $\mathbf{X}_{N\omega}^{(g,r)}$. Therefore, for any subsequence $\mathbf{X}_{N''\omega}^{(g,r)}$, we can choose a subsubsequence $\mathbf{X}_{N'''\omega}^{(g,r)}$ (VW Lemma 1.9.2(ii)) such that for almost all $\omega \in \Omega$,

$$\sup_{h \in \mathcal{B}} \left| \mathbb{E}_g \left[h \left(\mathbf{X}_{N'''\omega}^{(g,r)} \right) \right] - \mathbb{E} \left[h(\mathbf{G}) \right] \right| \xrightarrow{N'' \rightarrow \infty} 0. \tag{21}$$

Since $\hat{\mu}_N$ converges to μ \mathbb{P} -almost surely, there exists $\Omega' \subset \Omega$ with $\mathbb{P}(\Omega') = 1$ such that for all $\omega \in \Omega'$ it holds that $\hat{\mu}_{N''\omega} \rightarrow \mu$ as N'' tends to infinity and (21) holds. VW's Theorem 1.12.2 implies that $\mathbf{X}_{N'''\omega}^{(g,r)}$ converges in distribution for all $\omega \in \Omega'$. Hence Slutsky's Lemma implies that $dH_{\hat{\mu}_{N'''\omega}^{(r)}} \mathbf{X}_{N'''\omega}^{(g,r)} \rightsquigarrow \tilde{G}$ for all $\omega \in \Omega'$. A further application of VW's Theorem 1.12.2 yields

$$\sup_{h \in \mathcal{B}} \left| \mathbb{E}_g \left[h \left(dH_{\hat{\mu}_{N'''\omega}^{(r)}} \mathbf{X}_{N'''\omega}^{(g,r)} \right) \right] - \mathbb{E} \left[h(\tilde{G}) \right] \right| \rightarrow 0$$

for all $\omega \in \Omega'$. Since the subsequence N' was arbitrary the claim follows from eq. (20) and VW's Lemma 1.9.2(ii). \square

The usefulness of the above theorem is mainly due to the following corollary.

Corollary 3. *Given any continuous function $F : C(S) \rightarrow \mathbb{R}$, for every point $a \in \mathbb{R}$ at which $\mathbb{P}(F(\tilde{G}) \leq a)$ is continuous, we have that $\mathbb{P}\left(F\left(\tilde{G}_{N\omega}^{(g,r)}\right) \leq a\right) \rightarrow \mathbb{P}\left(F(\tilde{G}) \leq a\right)$ for almost all $\omega \in \Omega$.*

Proof. Suppose the claim is false, then there exists $a \in \mathbb{R}$ at which $\mathbb{P}(F(\tilde{G}) \leq a)$ is continuous, $\epsilon > 0$, $\tilde{\Omega} \subset \Omega$ with $\mathbb{P}(\tilde{\Omega}) > 0$ and a subsequence $(N_j)_{j \in \mathbb{N}}$ such that for all j , $|\mathbb{P}\left(F\left(\tilde{G}_{N_j\omega}^{(g,r)}\right) \leq a\right) - \mathbb{P}\left(F(\tilde{G}) \leq a\right)| > \epsilon$ for all $\omega \in \tilde{\Omega}$. Now, applying Theorem 3(ii) and Lemma 1.9.2(ii) from VW, it follows that there exists a subsubsequence $(N_{j_k})_{k \in \mathbb{N}}$ such that $\sup_{h \in \mathcal{B}} |\mathbb{E}_g[h(\tilde{G}_{N_{j_k}\omega}^{(g,r)})] -$

$\mathbb{E}_g[h(\tilde{G})]$ converges to 0 for almost all $\omega \in \Omega$. In particular by Theorem 1.12.2 in VW and the Continuous Mapping Theorem, $F\left(\tilde{G}_{N_{jk}\omega}^{(g,r)}\right)$ converges weakly to $F(\tilde{G})$. Hence $\mathbb{P}(\tilde{\Omega}) = 0$. This gives a contradiction. \square

Remark 5. The above corollary applies when F is the maximum norm $\|\cdot\|_\infty$. This means that the multiplier bootstrap consistently estimates the quantiles of the maximum, which we will use for the construction of simultaneous confidence bands in the next section.

Remark 6. The construction of functional delta residuals and the above multiplier theorem can be extended to converging sequences of transformations $(H_N)_{N \in \mathbb{N}} \subset C^1(\mathbb{R}^D, \mathbb{R})$ to a transformation $H \in C^1(\mathbb{R}^D, \mathbb{R})$. This requires that the gradients $\nabla H|_x, \nabla H_N|_x$ satisfy the following uniform convergence for some $\epsilon > 0$:

$$\lim_{N \rightarrow \infty} \max_{x \in D_{\mu^{(r)}}^\epsilon} |\nabla H_N|_x - \nabla H|_x| = 0 \quad (22)$$

with $D_{\mu^{(r)}}^\epsilon = \left\{ x \in \mathbb{R}^D : x = \mu^{(r)}(s) \pm \eta \text{ for some } s \in S, |\eta| \leq \epsilon \right\}$.

The proof that the functional delta method remains valid for such transformations can be found in 6. Moreover, the only change in the proof of Theorem 3 is that the extended continuous mapping theorem [Kosorok, 2008, Theorem 7.24] needs to be used.

3.5 Simultaneous Confidence Bands

Throughout this section we require that the assumption of Theorem 2 hold.

Construction of the SCBs Functional delta residuals can be applied to construct simultaneous confidence bands (SCBs) for $H(\mu^{(r)})$. The easiest way to do so is based on t -statistics (see e.g., Telschow and Schwartzman [2022]). To do so, in the context of moment-based statistics for $s \in S$ and a quantile $q_{\alpha, N} \in \mathbb{R}$, we define the collection of intervals SCB($s, N, q_{\alpha, N}$) with endpoints

$$H\left(\hat{\mu}_N^{(r)}(s)\right) \pm q_{\alpha, N} \text{se}\left[H\left(\hat{\mu}_N^{(r)}(s)\right)\right]. \quad (23)$$

The sample estimator $\hat{\mu}_N^{(r)}$ fulfills a fCLT, see Theorem 2. Moreover, since the paths of X are \mathcal{L}^2 -Hölder continuous, $\hat{\mu}_N^{(r)}$ is also strongly consistent, i.e., $\|\hat{\mu}_N^{(r)} - \mu^{(r)}\|_\infty \rightarrow 0$ almost surely by Lemma 1(b). The standard error of the estimator is given by

$$\text{se}\left[H\left(\hat{\mu}_N^{(r)}(s)\right)\right] = \sqrt{\mathbb{E}\left[H\left(\hat{\mu}_N^{(r)}(s)\right) - \mathbb{E}\left[H\left(\hat{\mu}_N^{(r)}(s)\right)\right]\right]^2}, \quad (24)$$

which, asymptotically, can be consistently estimated, by Corollary 1, using the sample variance of the functional delta residuals. The intervals given by eq. (23) are $(1 - \alpha)$ -SCBs, if the quantile $q_{\alpha, N}$ satisfies

$$\mathbb{P}\left(\max_{s \in S} \left| \frac{H\left(\hat{\mu}_N^{(r)}(s)\right) - H\left(\mu^{(r)}(s)\right)}{\text{se}\left[H\left(\hat{\mu}_N^{(r)}(s)\right)\right]} \right| > q_{\alpha, N}\right) = \alpha. \quad (25)$$

The desired $q_{\alpha, N}$ cannot be calculated easily in the finite sample because, in general, the standard error (24) for finite N is hard to estimate. However, asymptotically the same arguments

as in [Chang et al. \[2017\]](#), yield the following asymptotic $(1 - \alpha)$ -SCBs for $H(\boldsymbol{\mu}^{(r)})$ and the asymptotic quantile q_α can be estimated using the delta residuals (as we will discuss different approaches to estimating this later on in this section).

Theorem 4. *Under the assumptions of Theorem 2 we define q_α such that*

$$\mathbb{P} \left(\max_{s \in S} \left| \frac{\tilde{G}(s)}{\sqrt{\text{Var}[\tilde{G}(s)]}} \right| > q_\alpha \right) = \alpha, \quad (26)$$

where \tilde{G} is defined in Corollary 1. Then

$$\lim_{N \rightarrow \infty} \mathbb{P} \left(H(\boldsymbol{\mu}^{(r)}(s)) \in \text{SCB}(s, N, q_\alpha) \text{ for all } s \in S \right) = 1 - \alpha.$$

Proof. Apply Corollary 1 together with Slutsky's Lemma. \square

If H is non-linear then the estimator $H(\hat{\boldsymbol{\mu}}_N^{(r)})$ for $H(\boldsymbol{\mu}^{(r)})$ is biased for finite N . As such it is possible to define bias corrected SCBs (as discussed in [Liebl and Reimherr \[2019\]](#)) to improve the finite sample size coverage of the SCBs. To do so we define, for $s \in S$, their endpoints as

$$H(\hat{\boldsymbol{\mu}}_N^{(r)}(s)) - \text{bias} \left[H(\hat{\boldsymbol{\mu}}_N^{(r)}(s)) \right] \pm q_{\alpha, N} \text{se} \left[H(\hat{\boldsymbol{\mu}}_N^{(r)}(s)) \right]. \quad (27)$$

Using $\nabla^2 H$ to denote the Hessian of H , the bias can be approximated as follows, using a Taylor expansion of H around $\boldsymbol{\mu}^{(r)}$,

$$\begin{aligned} \text{bias} \left[H(\hat{\boldsymbol{\mu}}_N^{(r)}(s)) \right] &= \mathbb{E} \left[H(\hat{\boldsymbol{\mu}}_N^{(r)}(s)) \right] - H(\boldsymbol{\mu}^{(r)}(s)) \\ &\approx \mathbb{E} \left[\nabla H_{\boldsymbol{\mu}^{(r)}}(\hat{\boldsymbol{\mu}}_N^{(r)}(s) - \boldsymbol{\mu}^{(r)}(s)) + \frac{1}{2} \nabla^2 H_{\boldsymbol{\mu}^{(r)}}(\hat{\boldsymbol{\mu}}_N^{(r)}(s) - \boldsymbol{\mu}^{(r)}(s), \hat{\boldsymbol{\mu}}_N^{(r)}(s) - \boldsymbol{\mu}^{(r)}(s)) \right] \\ &= \frac{1}{2} \mathbb{E} \left[\nabla^2 H_{\boldsymbol{\mu}^{(r)}}(\hat{\boldsymbol{\mu}}_N^{(r)}(s) - \boldsymbol{\mu}^{(r)}(s), \hat{\boldsymbol{\mu}}_N^{(r)}(s) - \boldsymbol{\mu}^{(r)}(s)) \right] \\ &= \frac{1}{2} \sum_{k=1}^K \sum_{k'=1}^K \frac{\partial^2 H}{\partial s_k \partial s_{k'}}(\boldsymbol{\mu}^{(r)}(s)) \cdot \mathbb{E} \left[(\hat{\boldsymbol{\mu}}_N^{(r_k)}(s) - \boldsymbol{\mu}^{(r_k)}(s)) (\hat{\boldsymbol{\mu}}_N^{(r_{k'})}(s) - \boldsymbol{\mu}^{(r_{k'})}(s)) \right] \\ &= \frac{1}{2N} \sum_{k=1}^K \sum_{k'=1}^K \frac{\partial^2 H}{\partial s_k \partial s_{k'}}(\boldsymbol{\mu}^{(r)}(s)) \cdot \left(\boldsymbol{\mu}^{(r_k+r_{k'})}(s) - \boldsymbol{\mu}^{(r_{k'})}(s) \boldsymbol{\mu}^{(r_k)}(s) \right). \end{aligned} \quad (28)$$

In our simulations we use a simple plugin estimator based on the strongly consistent estimator $\hat{\boldsymbol{\mu}}_N^{(r)}$ from equation (28)

$$\widehat{\text{bias}} \left[H(\hat{\boldsymbol{\mu}}_N^{(r)}) \right] = \frac{1}{2N} \sum_{k=1}^K \sum_{k'=1}^K \frac{\partial^2 H}{\partial s_k \partial s_{k'}}(\hat{\boldsymbol{\mu}}_N^{(r)}) \cdot \left(\hat{\boldsymbol{\mu}}_N^{(r_k+r_{k'})} - \hat{\boldsymbol{\mu}}_N^{(r_{k'})} \hat{\boldsymbol{\mu}}_N^{(r_k)} \right). \quad (29)$$

to estimate the bias. Strong consistency of $\hat{\boldsymbol{\mu}}_N^{(r)}$ implies that this bias estimate is strongly consistent, too. Plugging it into the SCBs (27) yields our bias corrected SCBs.

Estimation of the quantile q_α We have described one approach to calculate the asymptotic quantile q_α , i.e., estimating it using the α -quantile of the maximum of the multiplier bootstrap process based on the functional delta residuals from Section 3.4. This is an adaptation of Chang et al. [2017] and Corollary 3 implies that this estimate is consistent for q_α .

A second approach assumes that the residuals have C^3 sample paths and utilizes the Gaussian kinematic formula, compare [Telschow and Schwartzman, 2022]. Here the quantile q_α is approximated by exploiting the fact that for large $u \in \mathbb{R}$,

$$\mathbb{P}\left(\max_{s \in S} \hat{G}(s) > u\right) \approx \mathcal{L}_0 \Phi^+(u) + \sum_{d=1}^D \mathcal{L}_d \rho_d(u),$$

as shown in Taylor et al. [2005]. Here $\hat{G}(s) = \tilde{G}(s) / \sqrt{\text{Var}[\tilde{G}(s)]}$. The functions $\rho_d(u) = (2\pi)^{-(d+1)/2} \mathcal{H}_{d-1}(u) e^{-u^2/2}$, $d = 1, \dots, D$, are the so-called Euler characteristic densities, where \mathcal{H}_d is the d -th Hermite polynomial and $\Phi^+(u) = \mathbb{P}(N(0, 1) > u)$. The coefficients $\mathcal{L}_0, \dots, \mathcal{L}_D$ are referred to as the Lipschitz-Killing curvatures of S , which are intrinsic volumes of S considered as a Riemannian manifold endowed with a Riemannian metric induced by \hat{G} [Adler and Taylor, 2009, Chapter 12]. In particular, $\mathcal{L}_0 = \chi(S)$ is the Euler characteristic of the set S , which is usually known. Given consistent estimators $\hat{\mathcal{L}}_1, \dots, \hat{\mathcal{L}}_D$ of the Lipschitz-Killing curvatures an estimate \hat{q}_α of q_α can be found by finding the largest u such that

$$\mathcal{L}_0 \Phi^+(u) + \sum_{d=1}^D \hat{\mathcal{L}}_d \rho_d(u) = \alpha.$$

Currently there are only a few works dealing with estimation of Lipschitz-Killing curvatures for nonstationary processes and arbitrary dimensional domains S , see Taylor and Worsley [2007], Telschow et al. [2020]. The estimators from the last two sources require residuals which asymptotically have the covariance structure of the limiting process \hat{G} . The functional delta residuals satisfy this, once we normalize them to have empirical variance 1. We refer the reader to Telschow and Schwartzman [2022] for more details on how to use the Gaussian kinematic formula to estimate quantiles for SCBs.

Testing Gaussianity using Skewness and Kurtosis It is well-known that confidence intervals can be inverted to tests, see for example Lehmann et al. [2005]. By the same reasoning, simultaneous confidence bands for skewness and kurtosis can be used to test whether a sample is Gaussian. In order to do so we compute the simultaneous confidence bands for the pointwise skewness and kurtosis given in equations (16) and (17) under the assumption of Gaussianity. Assume that $X_1, \dots, X_N \stackrel{i.i.d.}{\sim} X$ with X being a Gaussian process on S . Using the formulas for the sample variance of g_1^N and g_2^N from Fisher [1930], as well as $\mathbb{E}[g_1^N] = 0$ and $\mathbb{E}[g_2^N] = -6/(N+1)$ for Gaussian samples, Theorem 4 implies, if X is Gaussian, that for any $\alpha \in (0, 1)$

$$\begin{aligned} \lim_{N \rightarrow \infty} \mathbb{P}\left(\max_{s \in S} |g_1^N(s)| > q_\alpha^{(g_1^N)} \sqrt{\frac{6(N-2)}{(N+1)(N+3)}}\right) &= \alpha, \\ \lim_{N \rightarrow \infty} \mathbb{P}\left(\max_{s \in S} \left|g_2^N(s) + \frac{6}{N+1}\right| > q_\alpha^{(g_2^N)} \sqrt{\frac{24N(N-2)(N-3)}{(N+1)^2(N+3)(N+5)}}\right) &= \alpha. \end{aligned} \tag{30}$$

Here $q_\alpha^{(g_1^N)}$ and $q_\alpha^{(g_2^N)}$ are the quantiles obtained from applying Theorem 4 to g_1^N and g_2^N . Note that the only difference, with regards to the construction of the SCBs, is that we have replaced

the unknown standard error and the bias by the known Gaussian quantities. This shows that under the null hypothesis that X is Gaussian, the tests rejecting Gaussianity if

$$\begin{aligned} \max_{s \in S} |g_1^N(s)| &> q_\alpha^{(g_1^N)} \sqrt{\frac{6(N-2)}{(N+1)(N+3)}}, \\ \max_{s \in S} \left| g_2^N(s) + \frac{6}{N+1} \right| &> q_\alpha^{(g_2^N)} \sqrt{\frac{24N(N-2)(N-3)}{(N+1)^2(N+3)(N+5)}} \end{aligned} \quad (31)$$

are asymptotically exact. Hence either of the SCBs can be used to test departure for Gaussianity. The skewness SCBs check whether there is departure from Gaussianity due to significant non-zero skewness for any $s \in S$, while the excess kurtosis SCBs do the same for significant non-zero excess kurtosis.

In the simulations from Section 4 we will see that nominal coverage for the above bands requires very large N . This is partially because the rate of convergence of g_1^N and g_2^N to their asymptotic normal distributions is very slow. To solve this problem D'Agostino [1970] proposed a transformation making g_1 approximately standard normal for any $N \geq 8$ and Anscombe and Glynn [1983] proposed a transformation doing the same for g_2 for $N \geq 20$. For samples of real valued random variables D'agostino et al. [1990] argued that these transformations give powerful tests for Gaussianity. The transformation which is applied to g_1 is given by

$$\begin{aligned} Z_{1,N}(x) &= \frac{1}{\sqrt{\log(W_N)N}} \operatorname{asinh} \left(\frac{x}{\alpha_N \sqrt{c_{1,N}}} \right) \xrightarrow{N \rightarrow \infty} 0.335 \cdot \operatorname{asinh}(1.216 \cdot x), \\ W_N^2 &= \sqrt{2c_{2,N} - 2} - 1, \quad \alpha_N^2 = \frac{2}{W_N^2 - 1}. \end{aligned} \quad (32)$$

where $c_{1,N}$ and $c_{2,N}$ are constants depending only on N , which can be found in D'Agostino [1970]. The transformation which is applied to g_2 is given by

$$\begin{aligned} Z_{2,N}(x) &= \sqrt{\frac{9A_N}{2N}} \left(1 - \frac{2}{9A_N} - \left(\frac{1 - 2/A_N}{1 + \frac{x+3-b_{1,N}}{\sqrt{b_{2,N}}} \sqrt{2/(A_N-4)}} \right)^{1/3} \right) \xrightarrow{N \rightarrow \infty} 0.8165 \cdot \left(1 - \left(\frac{1}{1 + 0.75 \cdot (x + \dots)} \right) \right) \\ A_N &= 6 + \frac{8}{\sqrt{b_{3,N}}} \left(\frac{2}{\sqrt{b_{3,N}}} + \sqrt{1 + \frac{4}{b_{3,N}}} \right). \end{aligned} \quad (33)$$

Here $b_{1,N}$, $b_{2,N}$ and $b_{3,N}$ are again constants depending on N , which can be found in D'agostino et al. [1990].

The transformation $Z_{1,N}(g_1^N(s))$ of the sample skewness and the transformation $Z_{1,N}(g_1^N(s))$ of the sample excess kurtosis are both moment-based statistics and satisfy the assumptions from Remark 6 as is proven in 6. Since, under the assumption that X is Gaussian, the transformed estimators are unit-variance and zero-mean, we obtain asymptotic $(1-\alpha)$ -SCBs for the transformed skewness with endpoints

$$Z_{1,N}(g_1^N(s)) \pm q_\alpha^{Z_{1,N}(g_1^N)} \quad (34)$$

and therefore reject Gaussianity of the sample due to non-zero skewness, if zero is not contained in all of these intervals. Similarly, we can test departure of Gaussianity due to non-zero excess-kurtosis with the SCBs with endpoints

$$Z_{2,N}(g_2^N(s)) \pm q_\alpha^{Z_{2,N}(g_2^N)}. \quad (35)$$

Since these transformations are bijective for all $N \in \mathbb{N} \cup \{\infty\}$ the SCBs for the transformed variable can be turned into $(1-\alpha)$ -SCBs for skewness and excess kurtosis by applying their inverse. These SCBs might be easier to interpret.

4 Simulations of Coverage for Simultaneous Confidence Bands

In this section we study the coverage rate of simultaneous confidence bands for different moment-based statistics. We use 20,000 Monte Carlo simulations to assess the coverage and evaluate the processes on a grid of $[0, 1]$ composed of 175 equally spaced points. The bands are calculated as described in Section 3.5. In particular, the quantile q_α is estimated using either the functional delta residuals through the multiplier bootstraps given in Chang et al. [2017], Telschow and Schwartzman [2022] with Rademacher (rMult/rtMult) or Gaussian multipliers (Mult/tMult) using 5000 bootstrap replicates or the Gaussian kinematic formula (GKF/tGKF), see Section 3.5. Here the "t" for multiplier bootstraps denotes the t -multiplier bootstrap and tGKF refers to the Gaussian kinematic formula for a t -process rather than the Gaussian one, see e.g. Telschow and Schwartzman [2022]. We compare different constructions for the SCBs with and without the bias correction (eq. (29)). The results for bias correction (except for Cohen's d) are deferred to the appendix, since the coverage rates of the SCBs in general are closer to nominal without estimating the bias. In the Gaussian simulations the standard error (s.e.) for the moment-based statistics are known. Hence in such cases we compare SCBs using the known Gaussian s.e. and SCBs using the s.e. estimate obtained from the empirical variance of the functional delta residuals (12). If the known Gaussian s.e. is used, this is indicated in the titles of the plots by writing *Gaussian S.E.*. For the estimated s.e. we use *Estimated S.E.* in the titles.

4.1 Functional Models of the Simulations

We compare the following three models defined on $S = [0, 1]$:

$$\text{Model A : } Y^A(s) = \sin(4\pi s) \exp(-3s) + \frac{(1-s-0.4)^2 + 1}{6} \cdot \frac{\mathbf{a}^T \mathbf{K}^A(s)}{\|\mathbf{K}^A(s)\|}$$

$$\text{Model B : } Y^B(s) = (s-0.3)^2 + \frac{\sin(3\pi s) + 1.5}{6} \cdot Z_B(s)$$

$$\text{Model C : } Y^C(s) = \sin(4\pi s) \exp(-3s) + (1.5-s) \cdot Z_C(s)$$

with $\mathbf{K}^A(s)$ being a vector with entries $K_i^A(s) = \exp\left(-\frac{(s-x_i)^2}{2h_i^2}\right)$ for $x_i = i/21$ and $\mathbf{a} \sim N(0, I_{21 \times 21})$. Hence Model A is a smooth non-stationary Gaussian process. The error process Z_B is the zero-mean Gaussian process having the non-stationary modified Matern-type covariance $c_{Z_B}(s, t) = c(s, t) / \sqrt{c(s, s)c(t, t)}$ with

$$c(s, t) = 0.4^2 \left(2^{1-\nu_{ts}} / \Gamma(\nu_{ts})\right) \left(\sqrt{2\nu_{ts}} |t-s|\right)^{\nu_{ts}} K_{\nu_{ts}}\left(\sqrt{2\nu_{ts}} |t-s|\right),$$

where $\nu_{t,s} = 1 - 3\sqrt{\max(s, t)} / 4$, compare the simulation section in Liebl and Reimherr [2019]. This model has continuous but non-differentiable paths. Model C is a smooth non-Gaussian error process of the form $Z_C(s) = W(s) / \sqrt{\text{Var}[W(s)]}$ with

$$W(s) = \frac{\sqrt{2}}{6}(\eta_1 - 1) \sin(\pi s) + \frac{2}{3}(\eta_2 - 1)(s - 0.5), \quad \eta_1 \sim \chi_1^2, \quad \eta_2 \sim \text{Exponential}(1). \quad (36)$$

Examples of the sample paths of these processes can be found in Figure 3.

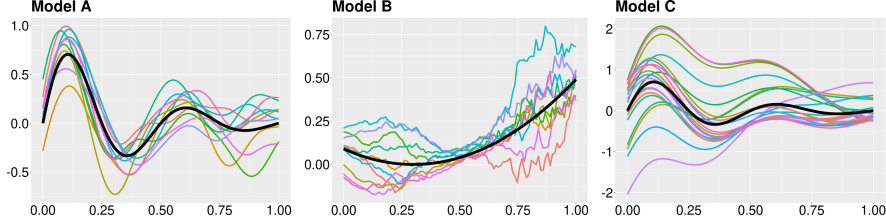


Figure 3: Examples of ten sample paths of the considered models. The bold black line is the true population mean.

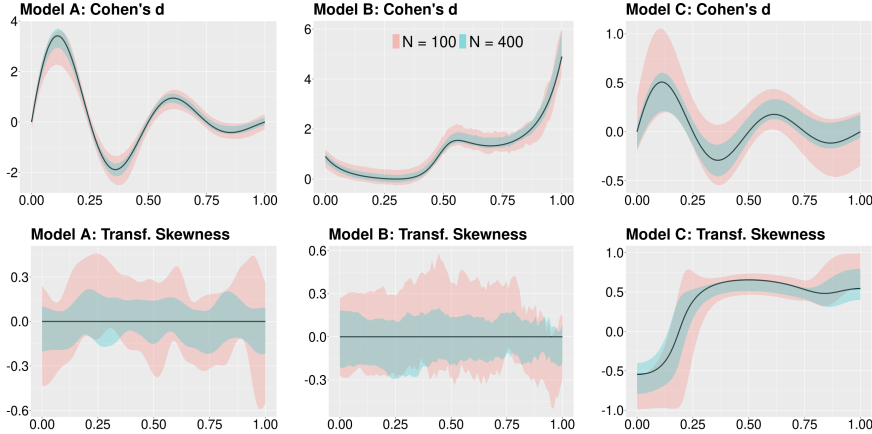


Figure 4: Examples of SCBs for moment-based statistics for two sample sizes. The bold black line is the true population parameter.

4.2 Coverage Rates for Cohen's d

Coverage rates of the SCBs for Model A are visualized in Figure 5. In this smooth Gaussian case the coverage rates are close to the nominal coverage rate of 0.95 for all methods of quantile estimation if N is larger than 200. The effect of estimating the bias is marginal. If the variance is estimated then all methods apart from the tGKF, require roughly $N = 400$ to converge to nominal coverage. The tGKF reaches nominal coverage for low sample sizes, which can be partly explained by the fact that the tGKF overestimates the coverage rates, if the true variance is known. The main cause of the slow convergence of the coverage rates is that the sample variance of the functional delta residuals substantially underestimates the true finite sample variance of the Cohen's d estimator for $N \leq 200$, compare Figure 10. The results for Model B are shown in Figure 6. They are similar to the results of Model A with the exception that the GKF and tGKF have over-coverage. This occurs because the GKF methods require C^2 sample paths. For the non-Gaussian model C the true variance of Cohen's d is not known. Hence we only simulated SCBs with estimated variances, see Figure 7. All methods, except those that use the GKF, have a coverage which converges asymptotically to the nominal level. The GKF approaches are slightly conservative. This holds because the EC heuristic for a Gaussian process X over an interval $S \subset \mathbb{R}$, used to justify the GKF, only gives an upper bound of the probability $\Pr(\max_{s \in S} X_s \geq u)$, see for example [Liebl and Reimherr \[2019\]](#).

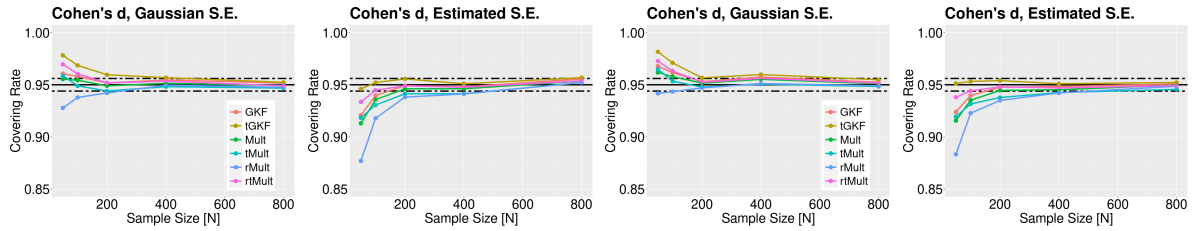


Figure 5: Simulations of coverage rates of SCBs for Model A. In the first two panels no bias correction is used in the construction of the SCBs, while in the third and fourth the coverage rate of bias-corrected SCBs is reported. The black dashed lines are 95% confidence intervals for the nominal level 0.95.

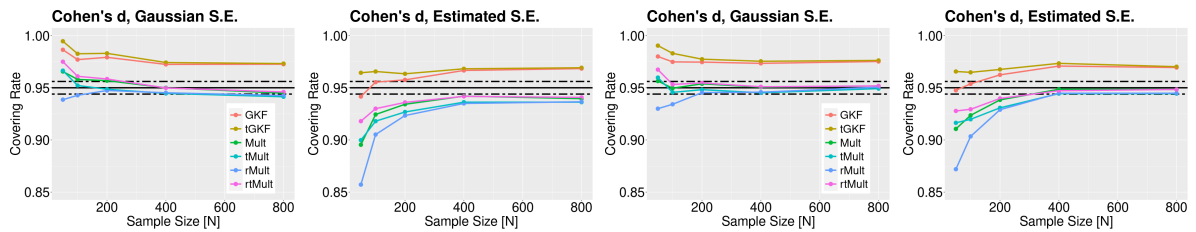


Figure 6: Simulations of coverage rates of SCBs for Model B. In the first two panels no bias correction is used in the construction of the SCBs, while in the third and fourth the coverage rate of bias-corrected SCBs is reported. The black dashed lines are 95% confidence intervals for the nominal level 0.95.

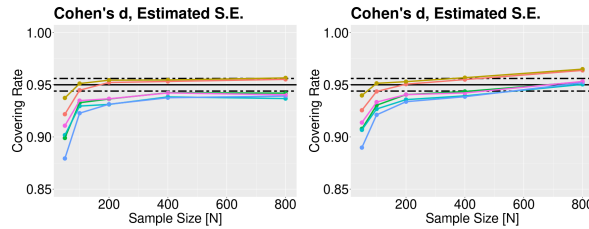


Figure 7: Simulations of coverage rates of SCBs for Model C. The first panels are the coverage rates of SCBs without the bias correction, while the second panel reports the coverage rate of bias-corrected SCBs. The black dashed lines are 95% confidence intervals for the nominal level 0.95.

4.3 Coverage Rates for Skewness and Kurtosis

For the smooth Gaussian Model A coverage rates of the SCBs for skewness and transformed skewness without including the bias estimate are shown in Figure 8. Transformed skewness means applying the additional transformation $Z_{1,N}$ to the moment-based statistic g_1 and constructing SCBs for the transformed parameter. Under Gaussianity the true transformed parameter is equal to zero for all $s \in S$. Convergence to nominal coverage of 0.95 for skewness requires sample sizes larger than $N \approx 800$ for all methods of quantile estimation. Only when the true finite sample size variance is used, a good level of coverage is achieved for sample sizes around $N \approx 400$, so long as the GKF or the Gaussian multiplier bootstrap is used for quantile estimation. The reason behind this is twofold.

First, Figure 10 shows that for finite N the estimated variances from the functional delta residuals underestimate the true finite N variance massively (up to 30% for $N = 50$) and only slowly converge to the correct finite sample variance of the skewness estimator. This problem is less severe for Cohen's d since the finite N variance is only slightly underestimated (up to 5% for $N = 50$). Hence finite sample coverage is improved, if we use the pre-knowledge of the true pointwise standard error of the skewness estimator under Gaussianity.

The second reason is that while the skewness estimator satisfies a fCLT, its convergence to a Gaussian process is slow. This can be remedied by using the transformed skewness parameter, which has a faster convergence to Gaussianity. In fact, SCBs for transformed skewness have almost exact coverage rates even for low N , if the true pointwise standard error of $1/\sqrt{N}$ for Gaussian samples is used. In particular, this shows that under the null hypothesis the test given in (34) for Gaussianity using the transformed skewness SCBs has the correct significance level of 0.05. Similar as for skewness using the pre-knowledge of the Gaussian variance is essential, since Figure 10 shows that estimating the variance correctly requires large N .

Furthermore, in both cases, bias estimation seems to reduce the coverage of the SCBs. Therefore these simulation results are deferred to the appendix. In general, it seems to be better to not account for the bias, which in the Gaussian case is zero for the pointwise skewness. Nevertheless, nominal coverage seems to be still reached for large N in all scenarios if the bias estimate is included into the construction of the SCBs. For the non-differentiable Model B , see Figure 9, the results are comparable to Model A except that once more the GKF methods have over-coverage for large N , since the sample paths of Model B are not C^2 and therefore do not satisfy the assumptions for the GKF methods.

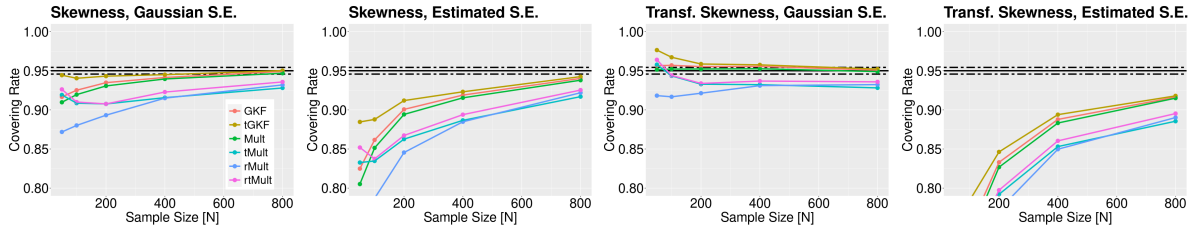


Figure 8: Simulations of coverage rates of SCBs for Model A . In these simulations no bias correction is applied. The black dashed lines are 95% confidence intervals for the nominal level 0.95. Special attention need to be placed on the third panel. It shows that the test for Gaussianity based on the SCBs for transformed skewness given in eq. (34) has the correct significance level even for small N for this Gaussian process so long as the GKF or Mult method is used for estimation of the quantile.

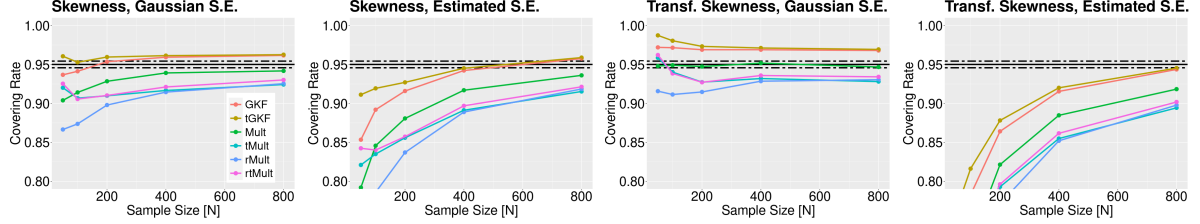


Figure 9: Simulations of coverage rates of SCBs for Model B . In these simulations no bias correction is applied. The black dashed lines are 95% confidence intervals for the nominal level 0.95. Special attention need to be placed on the third panel. It shows that the test for Gaussianity based on the SCBs for transformed skewness given in eq. (34) has the correct significance level even for small N for this Gaussian process so long as the Mult method is used for estimation of the quantile.

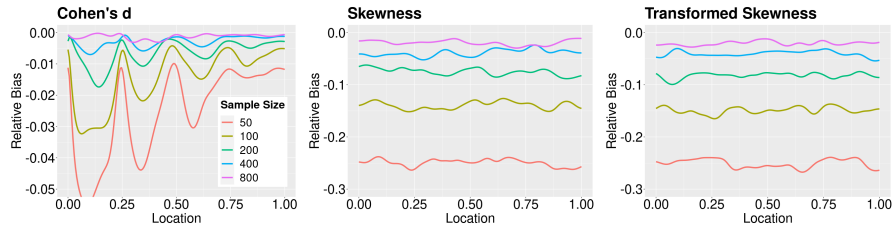


Figure 10: Dependency on sample size of the relative bias of s.e. estimates from the delta residuals for Model A . The colored curves are the estimates of the relative bias $\mathbb{E}[\text{estimated s.e.} - \text{true s.e.}] / (\text{true s.e.})$ obtained as the sample average of 5,000 Monte Carlo simulations.

Simulation results of coverage rates of the SCBs for kurtosis and transformed kurtosis for the Gaussian Models A and B are shown in Figure 11 and 12. They are fairly similar to the results for skewness. The main difference is that the coverage rates are lower and convergence to nominal requires larger N than in the case of skewness. Nevertheless, transforming kurtosis is again increasing coverage rates a lot such that even for low sample sizes we always have a coverage rate above 0.9. Simulation results for Model C can be found in 8.

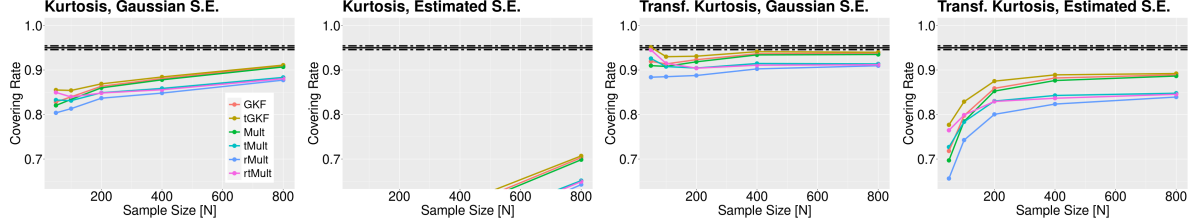


Figure 11: Simulations of coverage rates of SCBs for Model A . In these simulations no bias correction is applied. The black dashed lines are 95% confidence intervals for the nominal level 0.95. Special attention need to be placed on the third panel. It shows that the test for Gaussianity based on the SCBs for transformed kurtosis given in eq. (35) has a significance level that lies close to the nominal even for small N so long as the GKF or Mult method is used for estimation of the quantile.

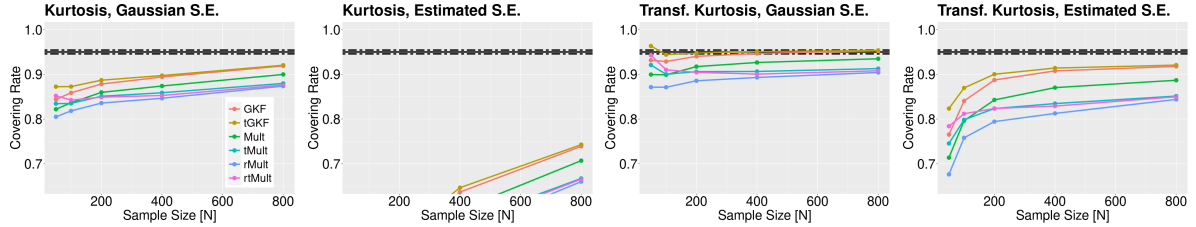


Figure 12: Simulations of coverage rates of SCBs for Model B . In these simulations no bias correction is applied. The black dashed lines are 95% confidence intervals for the nominal level 0.95. Special attention need to be placed on the third panel. It shows that the test for Gaussianity based on the SCBs for transformed kurtosis given in eq. (35) has a significance level that lies close to the nominal level even for small N as long as the GKF or Mult method is used for estimation of the quantile.

4.4 Coverage Rates for Skewness under Sampling and Observational Noise

In order to demonstrate the dependence of the coverage rates on additional observation noise and the density of the observed grid points, we simulated the coverage rate for the pointwise skewness estimator for $T \in \{50, 100, 175\}$ equidistant grid points of the interval $[0, 1]$. At each observed grid point we add iid zero-mean Gaussian noise with standard deviation 0.05 or 0.1. The observed noisy curves are smoothed using a local linear estimator, e.g., Degras [2011], where for each observed sample the smoothing bandwidth is obtained by cross-validation using `cv.select()` from the R-Package *SCBmeanfd* Degras [2016]. SCBs for the skewness parameter using the GKF and gMult are then constructed from the smoothed observations and it is checked whether they contain zero for all $t \in [0, 1]$. We decided to only report these two methods for the construction of SCBs, since the other bootstrap methods from the previous simulation perform similarly to before. The simulation results, shown in Figures 14, 15, 16 and 17, are similar to the results without observation noise and a dense observation grid from Figure 8 and 9, if the gMult approach is used. The construction based on the GKF has lower coverage for $T \in \{50, 100\}$. This is because estimation of the quantile using the tGKF relies on estimation of the variance of the derivative of the error process which is harder when the observations are less dense, since the estimation of these derivatives from the smoothed sample curves has a

larger bias.

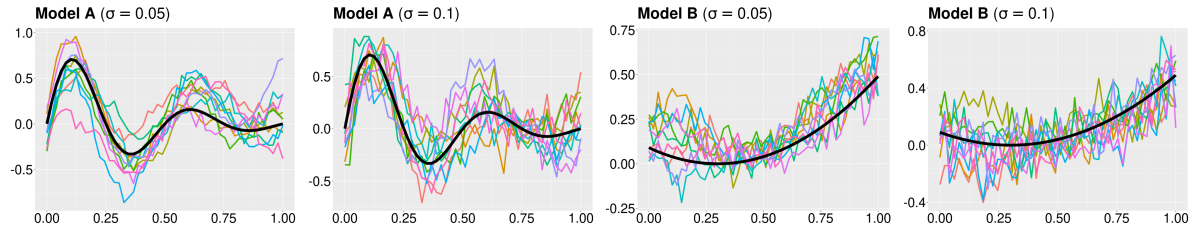


Figure 13: Samples of Model A and Model B with additive Gaussian observation noise. The bold black line is the true population mean.

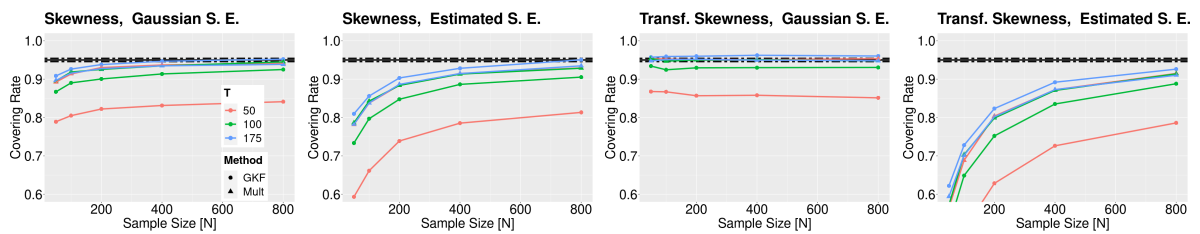


Figure 14: Dependency of coverage rate of SCBs for Model A with observation noise ($\sigma = 0.05$) on the number T of observation points. Panel 3 is again the most important since it shows that even in models with observation noise the significance level for a test for Gaussianity based on transformed skewness is close to the nominal so long as the sampling grid is sufficiently dense.

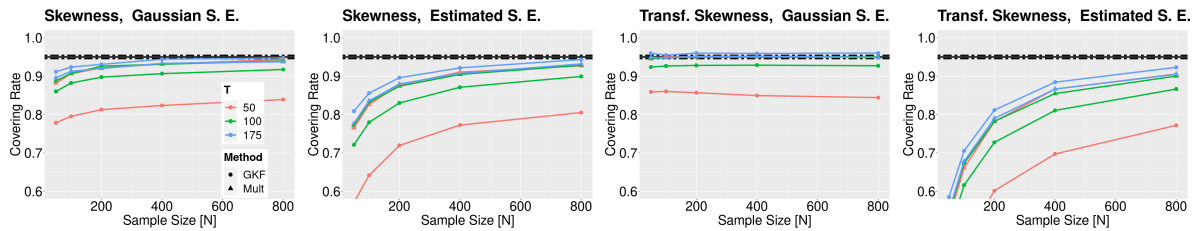


Figure 15: Dependency of coverage rate of SCBs for Model A with observation noise ($\sigma = 0.1$) on the number T of observation points. Panel 3 is again the most important since it shows that even in models with observation noise the significance level for a test for Gaussianity based on transformed skewness is close to the nominal so long as the sampling grid is sufficiently dense.

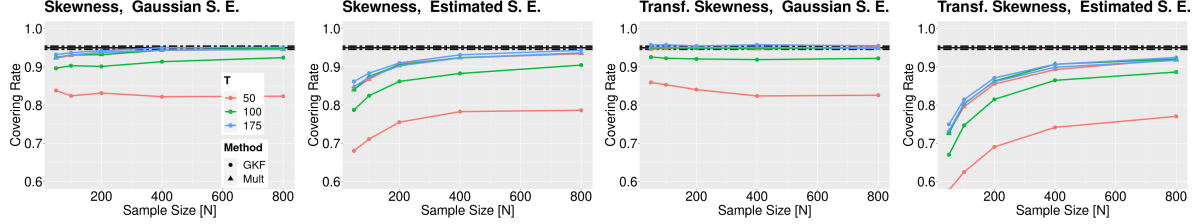


Figure 16: Dependency of coverage rate of SCBs for Model B with observation noise ($\sigma = 0.05$) on the number T of observation points. Panel 3 is again the most important since it shows that even in models with observation noise the significance level for a test for Gaussianity based on transformed skewness is close to the nominal so long as the sampling grid is sufficiently dense.

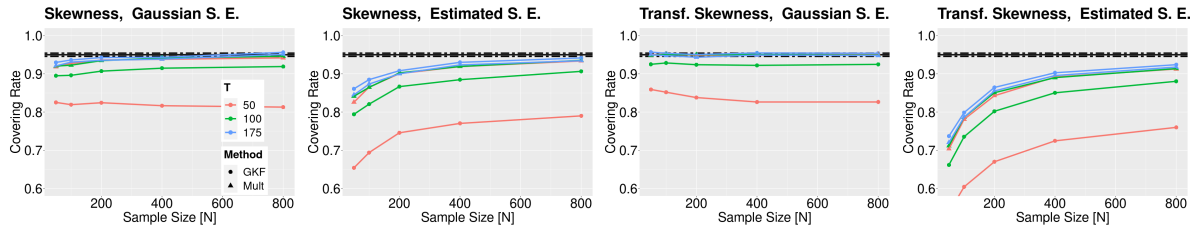


Figure 17: Dependency of coverage rate of SCBs for Model B with observation noise ($\sigma = 0.1$) on the number T of observation points. Panel 3 is again the most important since it shows that even in models with observation noise the significance level for a test for Gaussianity based on transformed skewness is close to the nominal so long as the sampling grid is sufficiently dense.

5 Discussion

Functional delta residuals are a powerful and helpful tool for performing inference on functional data. They are useful for extending spatial coverage probability excursion sets to effect-size measures, as demonstrated in [Bowring et al. \[2021\]](#), and for the construction of simultaneous confidence bands for Cohen’s d and other moment-based statistics, as done in this article. Moreover, as we have shown in Section 3.5 and our simulations such SCBs can be used to test Gaussianity of samples of a random field based on the transformed skewness or transformed kurtosis statistic.

The main challenge for the future is to improve upon the finite sample coverage for moment-based statistics. This in particular requires that the estimation of the standard error of moment-based statistics is improved. The empirical estimate obtained from the functional delta residuals, which converges asymptotically to the standard error of the moment-based statistic, suffers from the problem that the pointwise distributions of the functional delta residuals are heavily tailed and skewed due to the non-linear transformation. As such more robust estimators for the variance, than the standard sample variance estimator, might be required and could lead to faster convergence to nominal coverage.

Future research could extend the application of the functional delta residuals to other parameter estimators satisfying a fCLT derived from the functional delta method. Potential extensions are coverage probability excursion sets or simultaneous confidence bands for R^2 processes from linear models such as those usually fitted in functional magnetic resonance imaging analysis or new statistical methods such as LISA [\[Lohmann et al., 2018\]](#). The latter introduces spatial

smoothing of the z-score field of brain activation together with a false discovery rate controlled inference. In this context, any inference based on random field theory, e.g., cluster inference or coverage probability excursion sets, that is used to detect activation of the smoothed z-score process, will require residuals having the correct asymptotic correlation structure in order to perform valid inference. The functional delta residuals discussed in this article provide a tool to solve this problem.

Acknowledgments

F.T., S.D. and A.S. were partially supported by NIH grant R01EB026859. F.T. is also funded by the Deutsche Forschungsgemeinschaft (DFG) under Excellence Strategy The Berlin Mathematics Research Center MATH+ (EXC-2046/1, project ID:390685689).

References

- Holger Dette, Kevin Kokot, Alexander Aue, et al. Functional data analysis in the banach space of continuous functions. Annals of Statistics, 48(2):1168–1192, 2020.
- Holger Dette and Kevin Kokot. Bio-equivalence tests in functional data by maximum deviation. Biometrika, 2020.
- Robert J Adler. The geometry of random fields. Wiley, 1981.
- Keith J Worsley, Jonathan E Taylor, Francesco Tomaiuolo, and Jason Lerch. Unified univariate and multivariate random field theory. Neuroimage, 23:S189–S195, 2004.
- Jonathan E Taylor and Keith J Worsley. Detecting sparse signals in random fields, with an application to brain mapping. Journal of the American Statistical Association, 102(479): 913–928, 2007.
- David A Degras. Simultaneous confidence bands for nonparametric regression with functional data. Statistica Sinica, 21(4):1735–1765, 2011.
- Guanqun Cao, Lijian Yang, and David Todem. Simultaneous inference for the mean function based on dense functional data. Journal of Nonparametric Statistics, 24(2):359–377, 2012.
- Guanqun Cao. Simultaneous confidence bands for derivatives of dependent functional data. Electronic Journal of Statistics, 8(2):2639–2663, 2014.
- Chung Chang, Xuejing Lin, and R Todd Ogden. Simultaneous confidence bands for functional regression models. Journal of Statistical Planning and Inference, 188:67–81, 2017.
- Yueying Wang, Guannan Wang, Li Wang, and R Todd Ogden. Simultaneous confidence corridors for mean functions in functional data analysis of imaging data. Biometrics, 2019.
- Fabian JE Telschow and Armin Schwartzman. Simultaneous confidence bands for functional data using the gaussian kinematic formula. Journal of Statistical Planning and Inference, 216:70–94, 2022.
- Dominik Liebl and Matthew Reimherr. Fast and fair simultaneous confidence bands for functional parameters. arXiv preprint arXiv:1910.00131, 2019.

- Guanqun Cao, Li Wang, Yehua Li, and Lijian Yang. Oracle-efficient confidence envelopes for covariance functions in dense functional data. Statistica Sinica, pages 359–383, 2016.
- Jiangyan Wang, Guanqun Cao, Li Wang, and Lijian Yang. Simultaneous confidence band for stationary covariance function of dense functional data. Journal of Multivariate Analysis, 176:104584, 2020.
- Jia Guo, Bu Zhou, and Jin-Ting Zhang. Testing the equality of several covariance functions for functional data: A supremum-norm based test. Computational Statistics & Data Analysis, 124:15–26, 2018.
- Max Sommerfeld, Stephan Sain, and Armin Schwartzman. Confidence regions for spatial excursion sets from repeated random field observations, with an application to climate. Journal of the American Statistical Association, 113(523):1327–1340, 2018.
- Holger Dette and Kevin Kokot. Detecting relevant differences in the covariance operators of functional time series: a sup-norm approach. Annals of the Institute of Statistical Mathematics, pages 1–37, 2021.
- Alexander Bowring, Fabian Telschow, Armin Schwartzman, and Thomas E Nichols. Spatial confidence sets for raw effect size images. NeuroImage, 203:116187, 2019.
- Chung Chang and R Todd Ogden. Bootstrapping sums of independent but not identically distributed continuous processes with applications to functional data. Journal of multivariate analysis, 100(6):1291–1303, 2009.
- Robert J Adler and Jonathan E Taylor. Random fields and geometry. Springer Science & Business Media, 2009.
- Michael R Kosorok. Bootstraps of sums of independent but not identically distributed stochastic processes. Journal of Multivariate Analysis, 84(2):299–318, 2003.
- Alexander Bowring, Fabian JE Telschow, Armin Schwartzman, and Thomas E Nichols. Confidence sets for cohen’sd effect size images. NeuroImage, 226:117477, 2021.
- Samuel Davenport and Thomas E Nichols. Selective peak inference: Unbiased estimation of raw and standardized effect size at local maxima. Neuroimage, 209:116375, 2020.
- Ralph B D’agostino, Albert Belanger, and Ralph B D’Agostino Jr. A suggestion for using powerful and informative tests of normality. The American Statistician, 44(4):316–321, 1990.
- Michael R Kosorok. Introduction to empirical processes and semiparametric inference. Springer, 2008.
- Naresh C Jain and Michael B Marcus. Central limit theorems for $c(s)$ -valued random variables. Journal of Functional Analysis, 19(3):216–231, 1975.
- Henry J Landau and Lawrence A Shepp. On the supremum of a gaussian process. Sankhyā: The Indian Journal of Statistics, Series A, pages 369–378, 1970.
- James Davidson. Stochastic Limit Theory: An introduction for econometricians. OUP Oxford, 1994.

- Aad W Van Der Vaart and Jon A Wellner. Weak convergence and empirical processes. Springer, 1996.
- Patrick Billingsley. Convergence of probability measures. John Wiley & Sons, 1999.
- Simon N Vandekar and Jeremy Stephens. Improving the replicability of neuroimaging findings by thresholding effect sizes instead of p-values. Human Brain Mapping, 2021.
- Christophe Vignat. A generalized isserlis theorem for location mixtures of gaussian random vectors. Statistics & Probability Letters, 82(1):67–71, 2012.
- Derrick N Joanes and Christine A Gill. Comparing measures of sample skewness and kurtosis. Journal of the Royal Statistical Society: Series D (The Statistician), 47(1):183–189, 1998.
- Ronald A Fisher. The moments of the distribution for normal samples of measures of departure from normality. Proceedings of the Royal Society of London. Series A, Containing Papers of a Mathematical and Physical Character, 130(812):16–28, 1930.
- Jonathan Taylor, Akimichi Takemura, and Robert J Adler. Validity of the expected euler characteristic heuristic. The Annals of Probability, 33(4):1362–1396, 2005.
- Fabian Telschow, Armin Schwartzman, Dan Cheng, and Pratyush Pranav. Estimation of expected euler characteristic curves of nonstationary smooth gaussian random fields. arXiv preprint arXiv:1908.02493, 2020.
- Erich Leo Lehmann, Joseph P Romano, and George Casella. Testing statistical hypotheses, volume 3. Springer, 2005.
- Ralph B D’Agostino. Transformation to normality of the null distribution of g_1 . Biometrika, pages 679–681, 1970.
- Francis J Anscombe and William J Glynn. Distribution of the kurtosis statistic b_2 for normal samples. Biometrika, 70(1):227–234, 1983.
- David Degras. SCBmeanfd: Simultaneous Confidence Bands for the Mean of Functional Data, 2016. URL <https://CRAN.R-project.org/package=SCBmeanfd>. R package version 1.2.2.
- Gabriele Lohmann, Johannes Stelzer, Eric Lacosse, Vinod J Kumar, Karsten Mueller, Esther Kuehn, Wolfgang Grodd, and Klaus Scheffler. Lisa improves statistical analysis for fmri. Nature communications, 9(1):4014, 2018.
- Serge Lang. Real and functional analysis, volume 142. Springer Science & Business Media, 1993.

6 Auxiliary Lemmas

We now prove a small extension of the functional delta method (for example, [Kosorok, 2008, Theorem 2.8, p.235]) such that the transformation H can be a sequence of transformations H_N . Afterwards we will show that the transformations $Z_{1,N}$ and $Z_{2,N}$ satisfy the assumptions of the extended functional delta method.

Lemma 3. Assume that $(H_N)_{N \in \mathbb{N}} \subset C^1(\mathbb{R}^D, \mathbb{R})$ be a sequence and $H^1 \in C(\mathbb{R}^D, \mathbb{R})$. Let $\nabla H|_x, \nabla H_N|_x$ denote the gradients at $x \in \mathbb{R}^D$. For $\theta \in C(S, \mathbb{R}^D)$ define the set

$$D_\theta^\epsilon = \left\{ x \in \mathbb{R}^D : x = \theta(s) \pm \eta \text{ for some } s \in S, |\eta| \leq \epsilon \right\} \quad (37)$$

and assume that

$$\lim_{N \rightarrow \infty} \max_{x \in D_\theta^\epsilon} |\nabla H_N|_x - \nabla H|_x| = 0. \quad (38)$$

Let $r_N \rightarrow \infty$ and $(X_N)_{N \in \mathbb{N}} \subset C(S, \mathbb{R}^D)$ be a sequence of random fields such that

$$r_N(X_N - \theta) \rightsquigarrow X, \quad \text{in } C(S, \mathbb{R}^D) \quad (39)$$

with $X \in C(S, \mathbb{R}^D)$ being a limiting random field. Then

$$r_N(H_N(X_N) - H_N(\theta)) \rightsquigarrow \nabla H|_\theta X, \quad \text{in } C(S, \mathbb{R}^D) \quad (40)$$

Proof. We follow the idea of the proof of the functional delta method from [Kosorok, 2008, Theorem 2.8, p.235]. The key step is establishing

$$r_N(H_N(\theta + r_N^{-1}h_N) - H_N(\theta)) \rightarrow \nabla H|_\theta h \quad (41)$$

for all $h_N \in C(S, \mathbb{R}^D)$ satisfying $h_N \rightarrow h$ in $C(S, \mathbb{R}^D)$. Using Taylor's theorem we obtain

$$r_N(H_N(\theta + r_N^{-1}h_N) - H_N(\theta)) = \nabla H_N|_\theta h_N + \int_0^1 \left(\nabla H_N|_{\theta + yr_N^{-1}h_N} - \nabla H_N|_\theta \right) h_N dy, \quad (42)$$

see for example [Lang, 1993, p. 349f]. First note that

$$\left\| \nabla H_N|_\theta h_N - \nabla H|_\theta h \right\|_\infty \leq \left\| \nabla H_N|_\theta \right\|_\infty \left\| h_N - h \right\|_\infty + \left\| \nabla H_N|_\theta - \nabla H|_\theta \right\|_\infty \|h\|_\infty \quad (43)$$

converges to zero by (38). To see this note that $\left\| \nabla H_N|_\theta \right\|_\infty \rightarrow \left\| \nabla H|_\theta \right\|_\infty$ by inverse triangle inequality. For the second term we have for N large enough that

$$\begin{aligned} & \frac{1}{\|h_N\|_\infty} \max_{s \in S} \left| \int_0^1 \left(\nabla H_N|_{\theta(s) + yr_N^{-1}h_N(s)} - \nabla H_N|_{\theta(s)} \right) h_N(s) dy \right| \\ & \leq \max_{s \in S} \max_{y \in [0,1]} \left| \nabla H_N|_{\theta(s) + yr_N^{-1}h_N(s)} - \nabla H_N|_{\theta(s)} \right| \\ & \leq \max_{s \in S} \max_{y \in [0,1]} \left| \nabla H_N|_{\theta(s) + yr_N^{-1}h_N(s)} - \nabla H|_{\theta(s) + yr_N^{-1}h_N(s)} \right| \\ & \quad + \max_{s \in S} \max_{y \in [0,1]} \left| \nabla H|_{\theta(s) + yr_N^{-1}h_N(s)} - \nabla H|_{\theta(s)} \right| \\ & \quad + \max_{s \in S} \max_{y \in [0,1]} \left| \nabla H|_{\theta(s)} - \nabla H_N|_{\theta(s)} \right| \\ & \leq 2 \max_{x \in D_\theta^\epsilon} \left| \nabla H_N|_x - \nabla H|_x \right| + \max_{x \in D_\theta^\epsilon} \max_{|y| < \epsilon} \left| \nabla H|_x - \nabla H|_{x+y} \right| \end{aligned} \quad (44)$$

The first summand converges to zero by condition (38), the second can be made arbitrarily small, since as a continuous function $\nabla H|_x$ is uniform continuous on the compact set D_θ^ϵ . The rest of the proof follows Kosorok's proof. \square

Remark 7. It can be easily seen from the proof that (38) can be replaced with $(H_N)_{N \in \mathbb{N}} \subset C^2(\mathbb{R}^D, \mathbb{R})$ and

$$\lim_{N \rightarrow \infty} \max_{s \in S} |\nabla H_N|_{\theta} - \nabla H|_{\theta}| = 0 \quad \text{and,} \quad \sup_{N \in \mathbb{N}} \max_{x \in D_{\theta}^c} |\nabla^2 H_x| < \infty. \quad (45)$$

It remains to show that $Z_{1,N}$ and $Z_{2,N}$ satisfy the uniform convergence condition. Note that by the chain rule it is enough to show the assumptions only for these functions and not for the whole transformation which maps the moments to $Z_{1,N}(g_1)$, $Z_{2,N}(g_2)$ respectively.

Lemma 4. *Let $(a_N)_{N \in \mathbb{N}}$, $(b_N)_{N \in \mathbb{N}}$, $(c_N)_{N \in \mathbb{N}} \subset \mathbb{R}$ be sequences converging to $a, b, c \in \mathbb{R}$. Let $H \in C^1(\mathbb{R})$. Define the sequence of transformations to be $H_N(x) = a_N H(b_N x + c_N)$. Then for any compact set $D \subset \mathbb{R}$ it follows that*

$$\lim_{N \rightarrow \infty} \max_{x \in D} |H'_N|_x - aH'|_{bx+c}| = 0. \quad (46)$$

Proof. We compute:

$$\begin{aligned} |H'_N|_x - aH'|_{bx+c}| &= |a_N H'|_{b_N x + c_N} - aH'|_{bx+c}| \\ &\leq |a_N - a| |H'|_{b_N x + c_N}| + |a| |H'|_{b_N x + c_N} - H'|_{bx+c}|. \end{aligned} \quad (47)$$

Both summands converge to zero uniformly for all $x \in D$, since $|H'|_{b_N x + c_N}|$ is bounded on the compact set $b_N D c_N$ and since $|b_N x + c_N - bx + c| \leq |b_N - b| \max_{x \in D} |x| + |c_N - c|$ goes to zero uniformly and $H'|_x$ is uniform continuous on compact sets. \square

7 Bias corrected SCBs for Skewness and Kurtosis in Model A and Model B

In this section we report additional simulation results showing that bias correction in the construction of the SCBs for (transformed) skewness and (transformed) kurtosis in general does not improve the coverage rate of the SCBs, but rather decreases it. For the pointwise skewness estimator this is clear a priori for Gaussian data since the skewness estimator is unbiased. Therefore estimation of the bias only increases the variance. For transformed skewness, kurtosis and transformed kurtosis it is not immediately clear whether inclusion of the bias estimate is preferable. However, our simulations suggest that not including the bias estimate seems to be preferable. The other qualitative aspects of these simulations are very similar to the discussion of the SCBs from the simulation section of the main article.

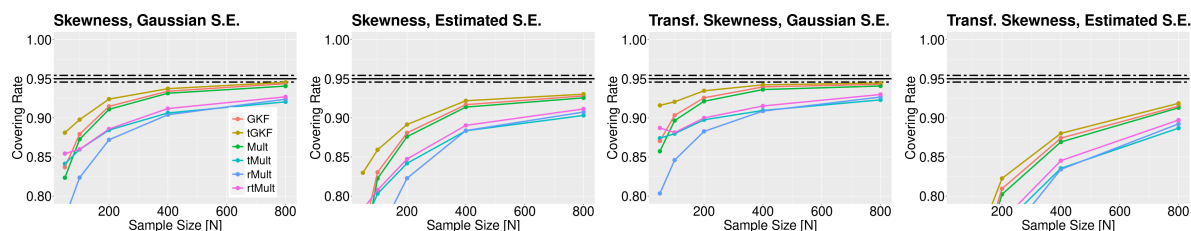


Figure 18: Simulations of coverage of bias corrected SCBs for skewness and transformed skewness for Model A. The black dashed lines are a 95% confidence intervals for the nominal level 0.95.

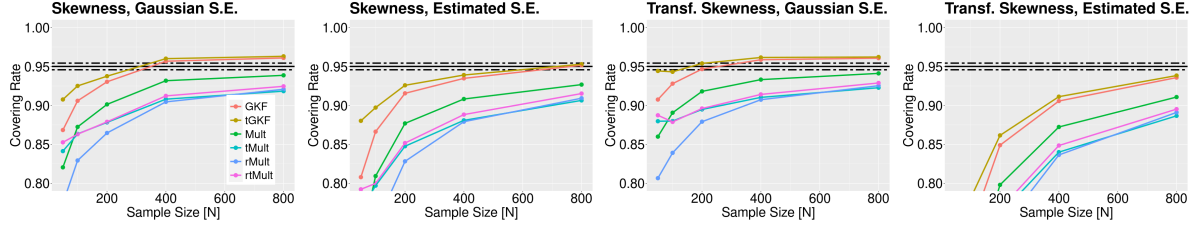


Figure 19: Simulations of coverage of bias corrected SCBs for skewness and transformed skewness for Model B. The black dashed lines are a 95% confidence intervals for the nominal level 0.95.

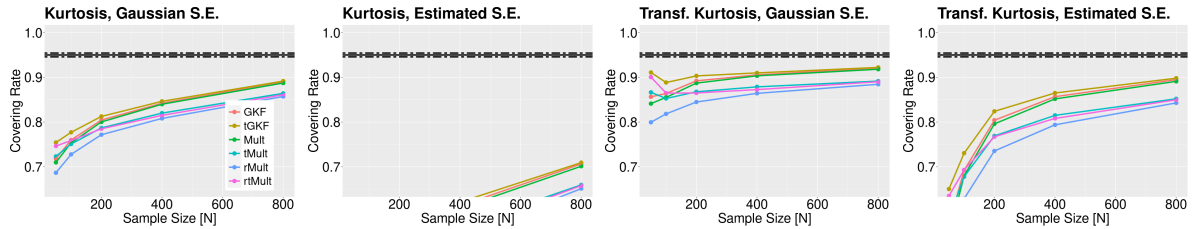


Figure 20: Simulations of coverage of bias corrected SCBs for kurtosis and transformed kurtosis for Model A. The black dashed lines are a 95% confidence intervals for the nominal level 0.95.

8 Simulations for SCBs for Skewness and Kurtosis in Model C

The simulations of coverage rates of SCBs for Model C for (transformed) skewness and (transformed) kurtosis are reported in Figures 22 and 23. Here we do not report simulations using the Gaussian standard error since it results in very low coverage rates. The pointwise standard errors of (transformed) skewness and (transformed) kurtosis for Model C are very different from the exact Gaussian quantities due to the high non-Gaussianity of Model C. As shown in Figures 22 and 23 the SCBs using the estimated standard error from the delta residuals require N to be much larger than 800 to converge to the nominal value. This is partially because the variance estimate of the skewness estimator requires even longer to converge under the non-Gaussian noise model than for Gaussian models. A solution for this extreme case to construct SCBs is left for future work.

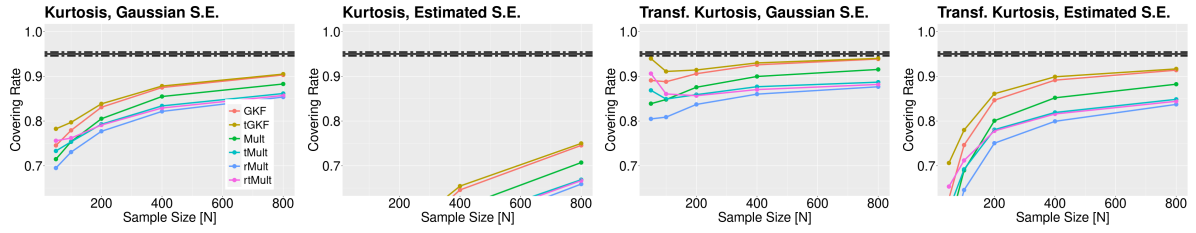


Figure 21: Simulations of coverage of bias corrected SCBs for kurtosis and transformed kurtosis for Model B. The black dashed lines are a 95% confidence intervals for the nominal level 0.95.

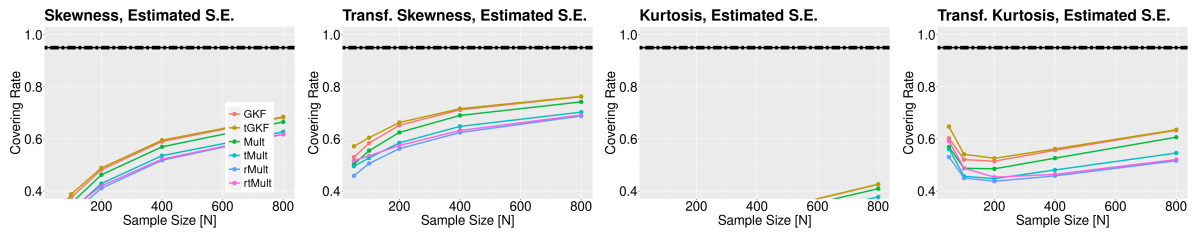


Figure 22: Simulations of coverage rates of SCBs for Model C. In these simulations no bias correction is applied. The black dashed lines are 95% confidence intervals for the nominal level 0.95.

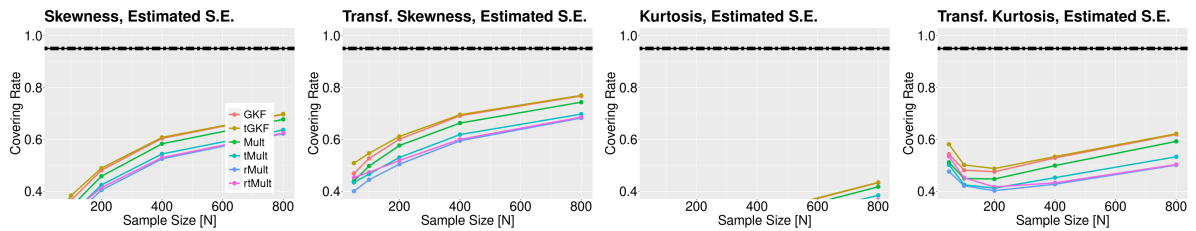


Figure 23: Simulations of coverage of SCBs for skewness, transformed skewness, kurtosis and transformed kurtosis (from left to right) for Model C. The black dashed lines are a 95% confidence intervals for the nominal level 0.95.